Chemical Probes for Bioimaging

Part 2: Sensor proteins for applications in research and diagnostics

Kai Johnsson

Department of Chemical Biology
Max Planck Institute for Medical Research, Heidelberg

Institute of Chemical Sciences and Engineering
EPFL, Lausanne

A comprehensive and excellent review on fluorescent biosensors

Genetically Encoded Fluorescent Biosensors Illuminate the Spatiotemporal Regulation of Signaling Networks
Eric C. Greenwald, Sohum Mehta*, and Jin Zhang*

https://pubs.acs.org/doi/10.1021/acs.chemrev.8b00333

Measuring the intracellular concentration of ATP

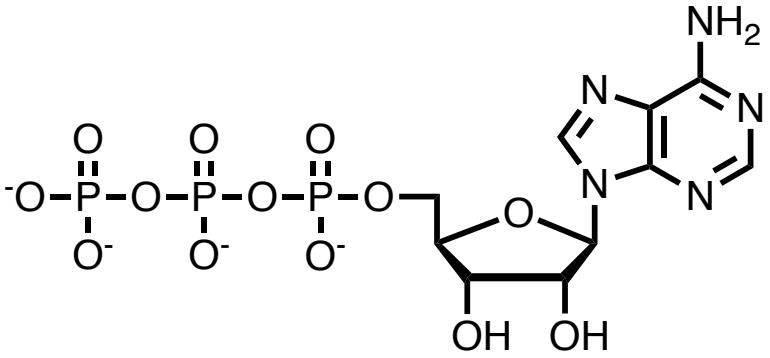

Visualization of ATP levels inside single living cells with fluorescence resonance energy transfer-based genetically encoded indicators

- See pdf of paper for better resolution version of figures shown in the following slides
- Reference of paper: http://www.ncbi.nlm.nih.gov/pubmed/19720993

Structure of ATP synthase

Composition F_1: (α_3, β_3, γ, δ, ε)

Composition F_0: 10-14 subunits **c** and one subunit **a**

F_0 is inserted into the membrane whereas F_0 and F_1 can be dissociated from the complex and be purified

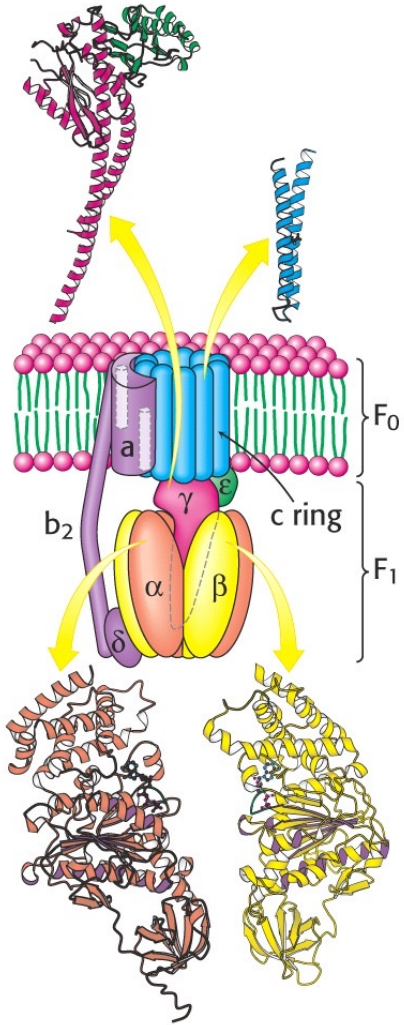

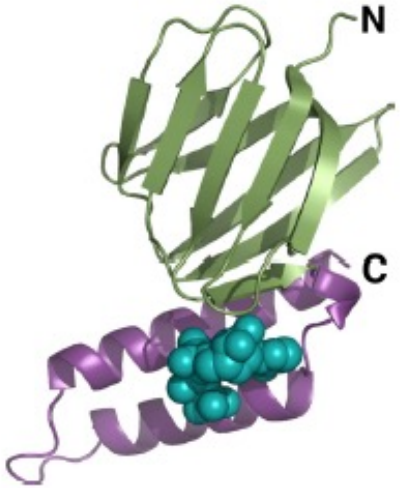

Fig. 1. Three-dimensional structure of *Bacillus* sp. PS3 ε subunit complexed with ATP (14). The N-terminal β-sandwich domain (residues 1–84) and C-terminal α-helical domain (residues 85–133) are colored green and magenta, respectively. ATP is represented as a cyan sphere model.

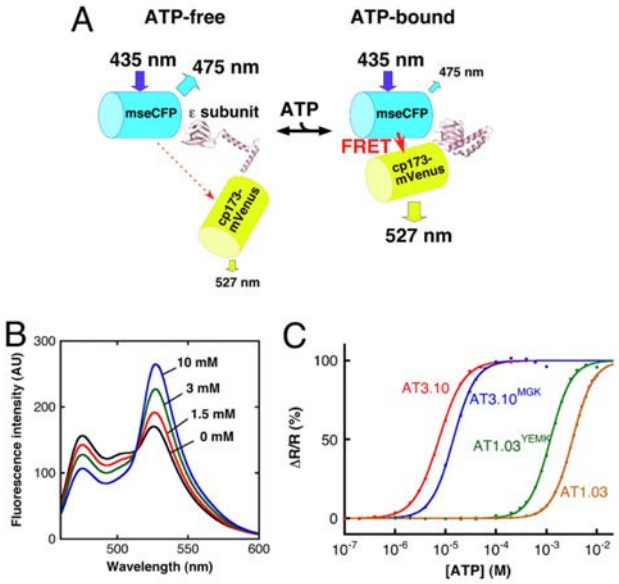

Fig. 2. FRET-based ATP probes, ATeam. (*A*) Schematic drawing of AT1.03 probe. Variants of CFP (mseCFP) and YFP (cp173-mVenus) were connected by the ε subunit of *Bacillus subtilis* F_oF_1-ATP synthase. In the ATP-free form (left), extended and flexible conformations of the ε subunit separate the two fluorescent proteins, resulting in low FRET efficiency. In the ATP-bound form, the ε subunit retracts to draw the two fluorescent proteins close to each other, which increases FRET efficiency. (*B*) ATP-dependent fluorescence spectral change of AT1.03 in vitro. Fluorescence emission of AT1.03 proteins at various ATP concentrations ([ATP]) and at 37 °C in 50 mM Mops-KOH (pH 7.3), 50 mM KCl, 0.5 mM $MgCl_2$, and 0.05% Triton X-100 was measured by exciting with 435 nm light. (*C*) ATP-dependent fluorescence emission ratio (R) changes of four ATeam proteins in vitro. The fraction of emission ratio (527/475 nm) change was plotted against [ATP]. Fluorescence of ATeam proteins was measured as in (*B*). Plots were fitted using a Hill equation: $\Delta R/R = \Delta R \times [ATP]^n/([ATP]^n + K_d^n)$. The apparent dissociation constant (K_d) and Hill coefficient (n) were calculated to be 7.4 μM and 1.7 (AT3.10), 14 μM and 2.0 (AT3.10MGK), 1.2 mM and 2.1 (AT1.03YEMK), and 3.3 mM and 2.1 (AT1.03), respectively.

Dependency of FRET efficiency **E** on distance **d** between the fluorophores and their orientation:

$$E = \frac{(R_o)^6}{(R_o)^6 + d^6}$$

$$(R_o)^6 = \frac{9\,(\ln 10)(\kappa^2 n^{-4}\, Q_o\, J)}{128\,\Pi^5\, N_A}$$

R_o = Förster distance; usually between 3-7 nm.

κ^2 = "Kappa square", the orientation factor. The value depends on the emission dipole moment of the donor (D-direction); the absorption transition dipole moment of the acceptor (A-direction); and the line connecting the centers of the donor fluorophore and the acceptor chromophore (R-direction) (see graph). κ^2 can have values between 0 and 4. The value 4 is achieved when both D and A are parallel or antiparallel to R. For freely rotating fluorophores $\kappa^2 = 2/3$.

Q_o = Quantum yield of donor fluorophore in the absence of acceptor

J = Spectral overlap integral of donor emission and acceptor absorption.

n = refractive index

N_A = Avogadro's number 6.022×10^{23}

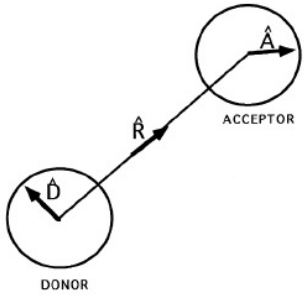

Fig. 1. The unit vectors $\hat{D}$, $\hat{A}$ and $\hat{R}$ are along the D-, A- and R-directions, respectively. $\hat{D}$ is along the emission transition moment of the donor, $\hat{A}$ is along the absorption transition moment of the acceptor, and $\hat{R}$ is along the line from the center of the donor fluorophore to that of the acceptor chromophore. $\hat{D}$, $\hat{A}$ and $\hat{R}$ can lie in one plane, but are in general not co-planar.

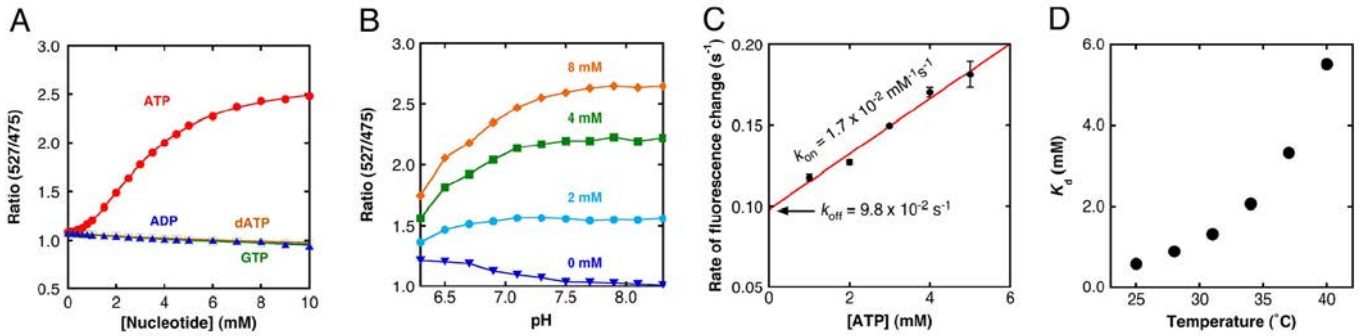

Fig. 3. Characterization of purified AT1.03 in vitro. (*A*) Nucleotide selectivity of AT1.03. The fluorescence emission ratio (527/475 nm) at 37 °C was plotted against nucleotide concentrations. Red filled circle, ATP; blue filled circle, ADP; green open square, GTP; orange open circle, dATP. Plots were fitted with Hill equations; $R = (R_{max} - R_{min}) \times [S]^n/([S]^n + K_d^n) + R_{min}$, where R_{max} and R_{min} are the maximum and minimum fluorescence ratios, respectively, K_d is the apparent dissociation constant, and n is a Hill coefficient. (*B*) pH dependence of AT1.03. The fluorescence ratios (527/475 nm) at 37 °C at 0, 2, 4, and 8 mM ATP in the pH range of 6.3–8.3 are shown. The buffer contained 50 mM Mops-KOH (pH 6.3–7.5) or Hepes-KOH (pH 7.7–8.3), 50 mM potassium chloride, 0.5 mM magnesium chloride, and 0.05% Triton X-100. (*C*) Reaction rate constants of AT1.03. Apparent rate constants ($k^{app} = k_{on}[ATP] + k_{off}$) at 37 °C, which were determined by fitting the CFP fluorescence decrease after ATP addition with a single exponential equation, were plotted against ATP concentrations ([ATP]). From a linear fit to the plot, k_{on} and k_{off} were calculated as 1.7×10^{-2} $mM^{-1}s^{-1}$ and 9.8×10^{-2} s^{-1}, respectively. (*D*) Dependence of K_d on temperature. K_d values for ATP were measured as in (*A*) at 25, 28, 31, 34, 37, and 40 °C.

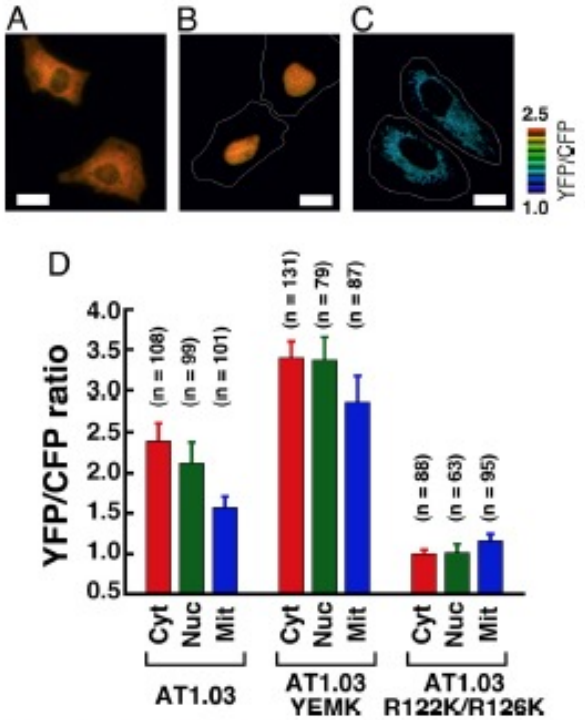

Fig. 4. Comparison of ATP concentrations ([ATP]) between different cellular compartments. (*A–C*) Expression of ATeam in different cellular compartments. Ratiometric pseudocolor images of AT1.03 expressed in cytoplasm (*A*), nucleus (*B*), and mitochondria (*C*) of HeLa cells. White lines represent cell outline. (Scale bar, 20 μm.) (*D*) Comparison of YFP/CFP emission ratio of ATeams in different cellular compartments. Three ATeams (AT1.03, AT1.03^{YEMK}, AT1.03$^{R122K/R126K}$), which have different affinity to ATP, were expressed in cytoplasm, nucleus, or mitochondria of HeLa cells. The ratio was calculated from fluorescent images. The numbers of cells used for calculating the ratio are indicated. Error bars are standard deviation of ratios.

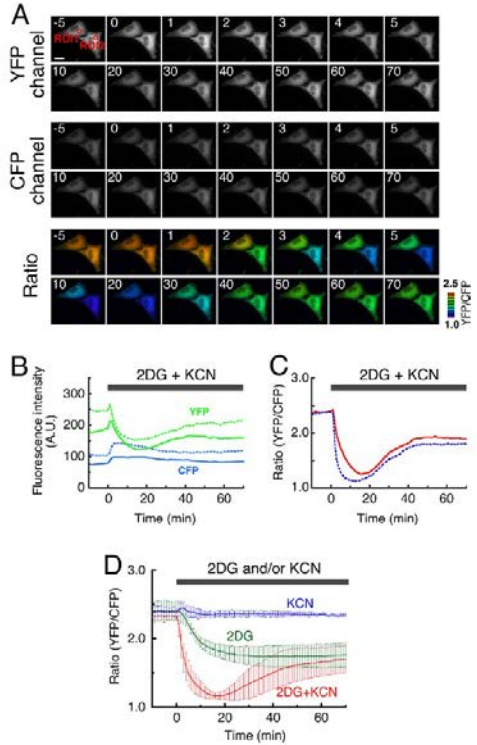

Fig. 5. Monitoring of cytoplasmic ATP levels of HeLa cells. (*A*) Sequential wide-field images of YFP (top), CFP (middle) and YFP/CFP emission ratio (bottom, pseudocolored) of a HeLa cell expressing AT1.03. Inhibitors of glycolysis (10 mM 2-deoxyglucose [2DG]) and OXPHOS (1 mM potassium cyanide [KCN]) were added at time = 0 (min). Elapsed time (in minutes) after addition of the inhibitors is shown to the top left of the cells. Images were obtained at 37 °C. (Scale bar, 20 μm). (*B*) Time course of fluorescence intensity of CFP (blue) and YFP (green) inside ROI1 (solid line) and ROI2 (dashed line) depicted in the top-left image of (*A*). (*C*) Time course of YFP/CFP emission ratio inside ROI1 (red solid line) and ROI2 (blue dashed line) depicted in the top-left image of (*A*). (*D*) Time course of averaged YFP/CFP emission ratio of HeLa cells expressing AT1.03. 2DG and/or potassium azide was added at time = 0 (min). Red, 2DG and KCN (n = 5); green, 2DG (n = 6); blue, KCN (n = 4). Error bars are standard deviations between measurements.

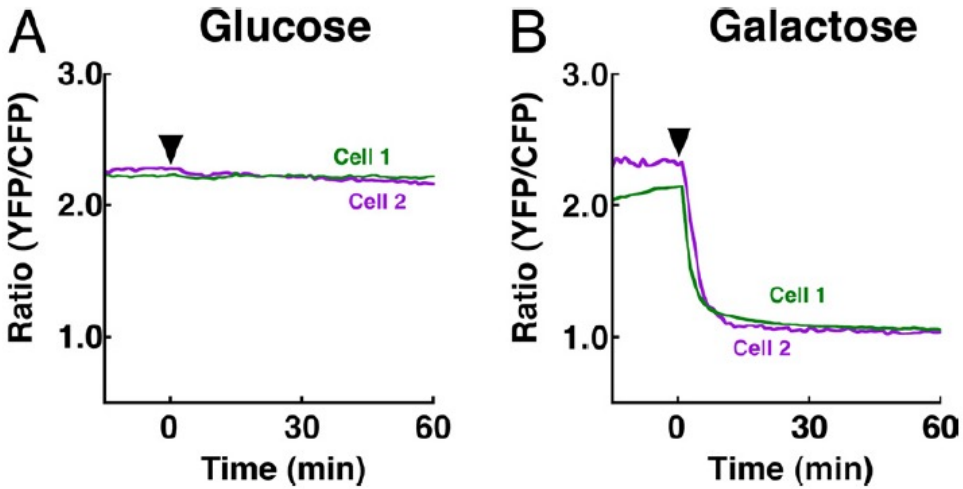

Fig. 6. Nutrient dependent alternation of ATP-generating pathway of HeLa cells. Sensitivity of intracellular ATP level to an OXPHOS inhibitor, oligomycin A, was examined for HeLa cells grown in glucose (*A*) or galactose (*B*) medium. Time courses of YFP/CFP emission ratio of cells expressing AT1.03, which were grown in DMEM without pyruvate containing 10 mM glucose (*A*) or 10 mM galactose (*B*), were monitored as in Fig. 5. Oligomycin A (10 μg/ml) was added to the medium at a time indicated by an arrow head.

Snifits: semisynthetic fluorescent sensor proteins

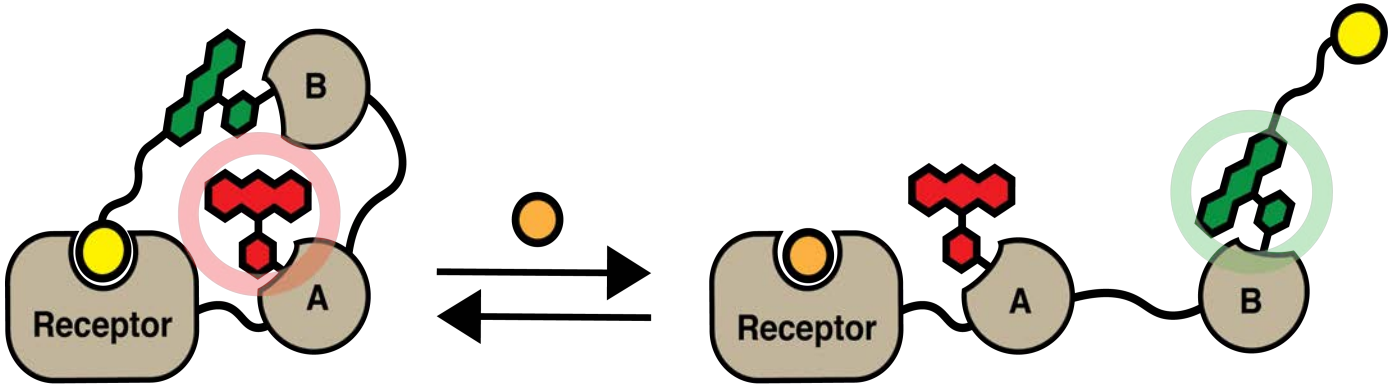

Snifits: semisynthetic fluorescent sensor proteins

Semisynthesis of Snifits

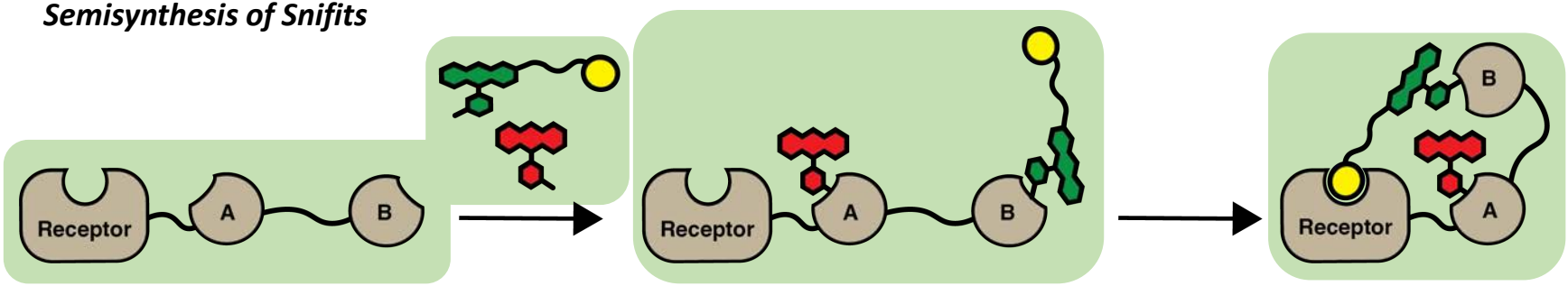

Sensing with Snifits

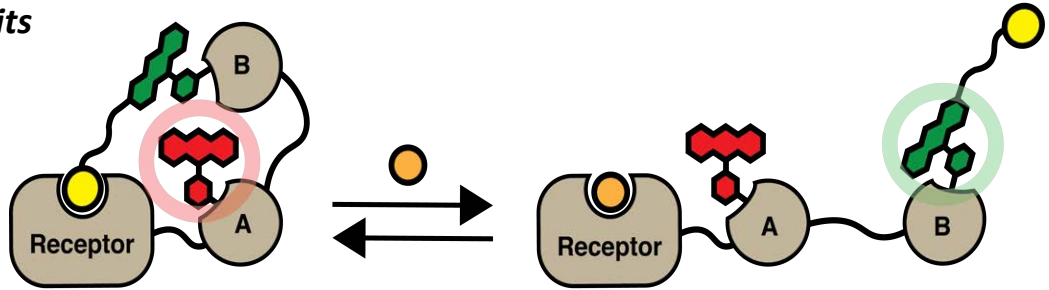

MAX-PLANCK-GESELLSCHAFT

Self-labeling proteins

SNAP-tag

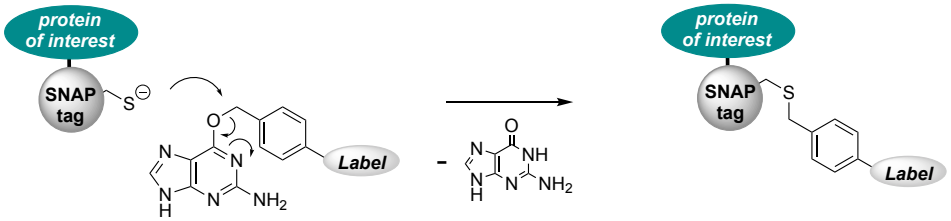

Keppler et al. Nature Biotech. **2003**, *21*, 86;

CLIP-tag

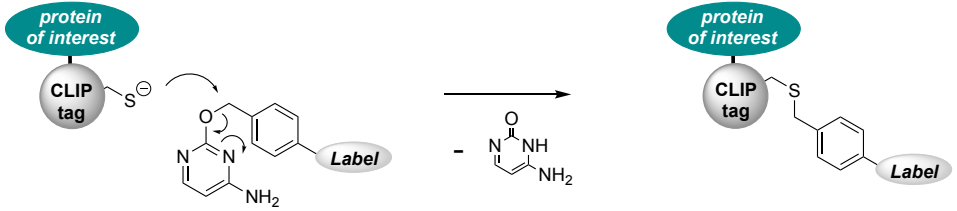

Gautier et al. Chem. Biol. **2008**, *15*, 128;

Halo-tag

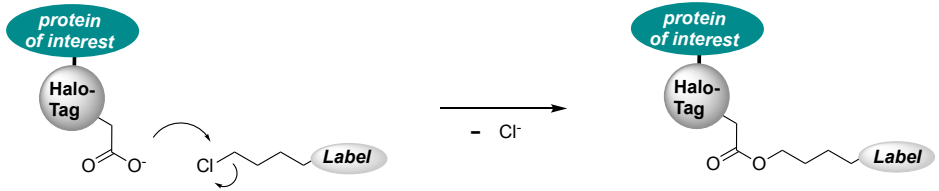

Los et. al. ACS Chem. Biol., **2008**, *3*, 373

MAX-PLANCK-GESELLSCHAFT

Glu-Snifit for sensing glutamate

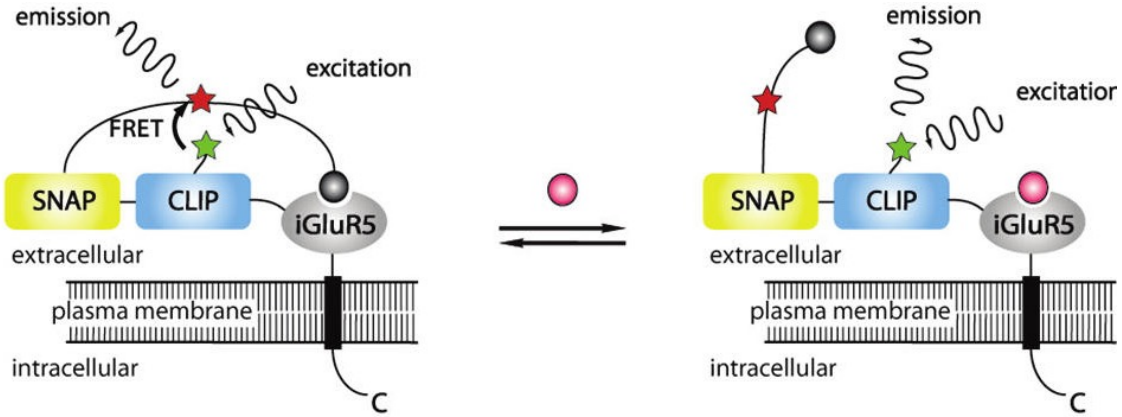

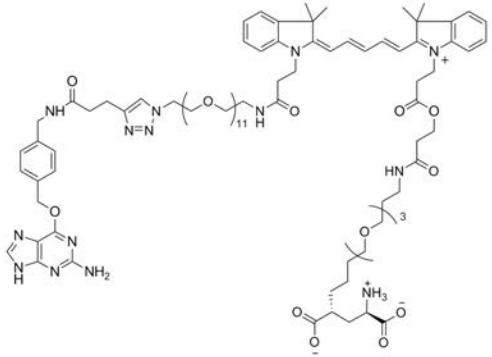

J Am Chem Soc **134**, 7676 (2012)

Snifits: competitive or cooperative binding of tethered ligand

Competitive binding

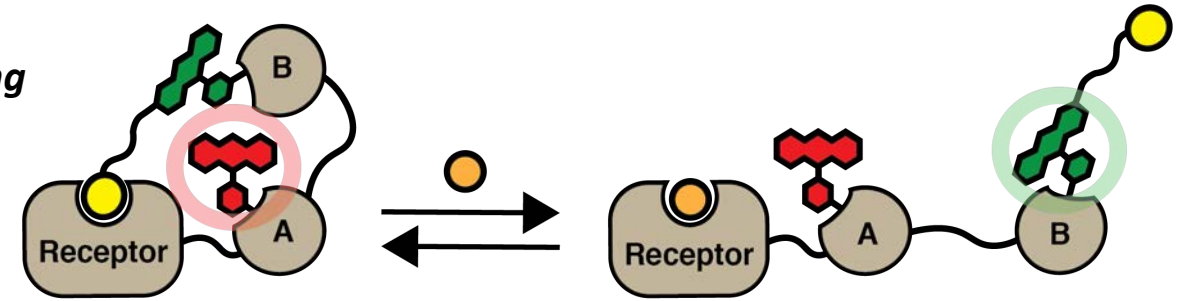

Cooperative binding

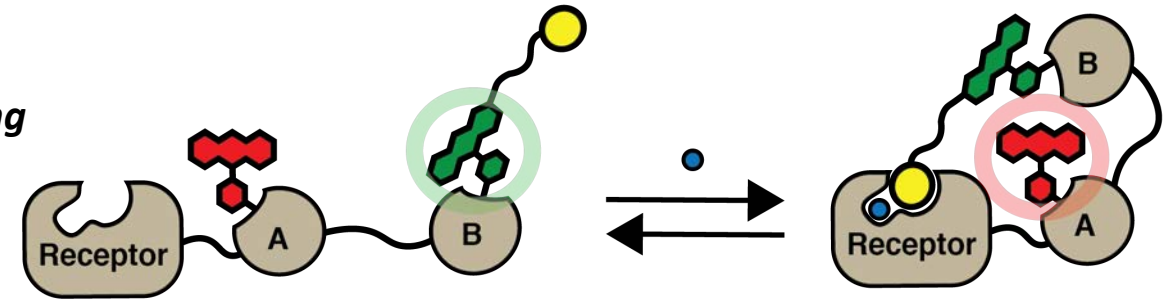

MAX-PLANCK-GESELLSCHAFT

Snifits based on unnatural amino acid technology

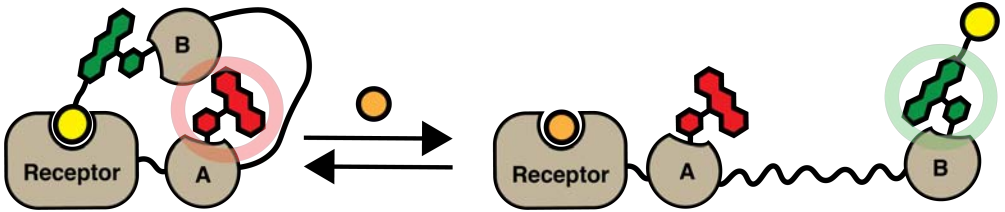

low FRET *even lower FRET*

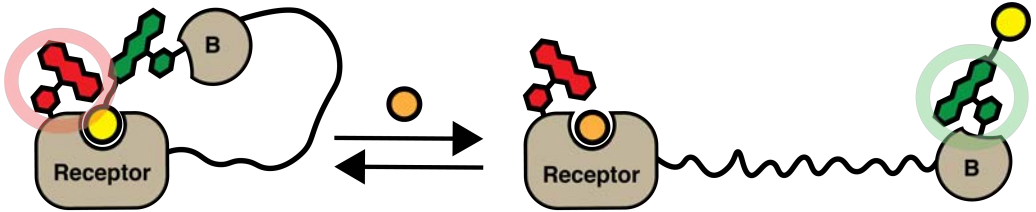

high FRET *low FRET*

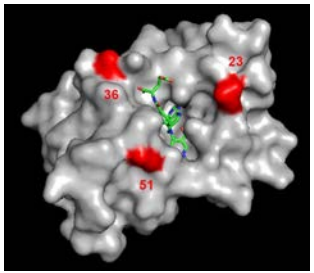

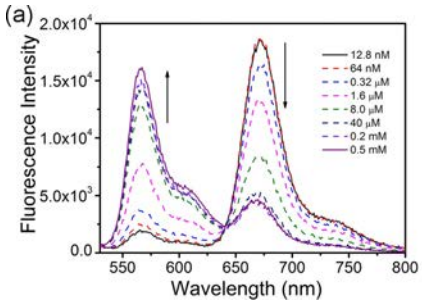

From FRET to BRET: Turning Snifits into Luciferase-based indicators

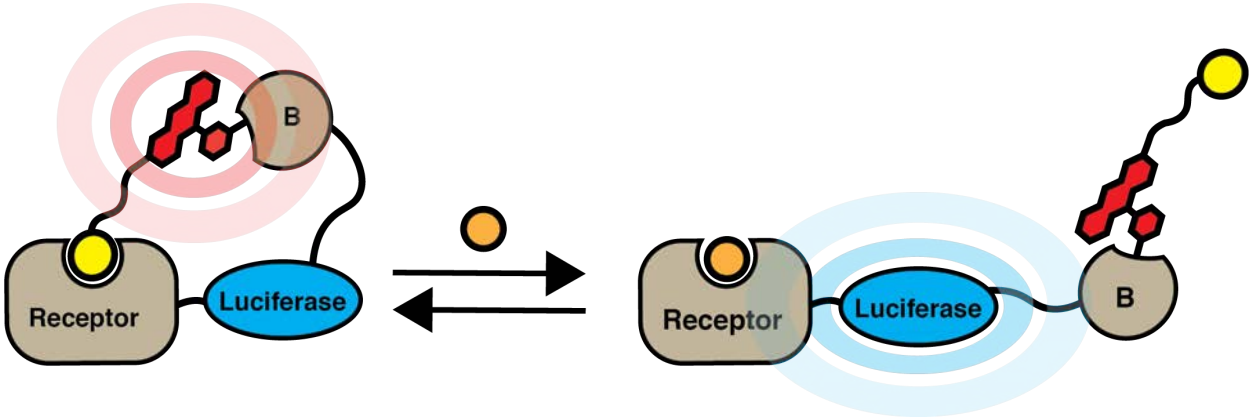

Nat Chem Biol **10**, 598 (2014)

Paper-based BRET assays

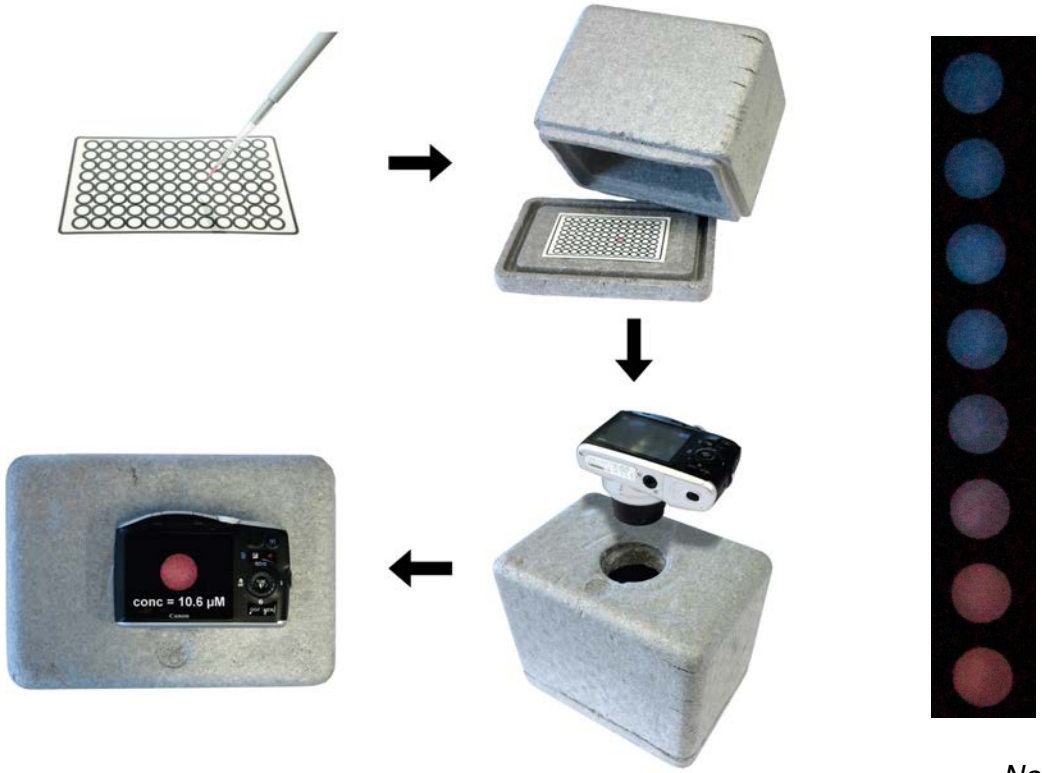

Nat Chem Biol **10**, 598 (2014)

Turning antibodies into Snifits; semisynthetic bioluminescent antibodies

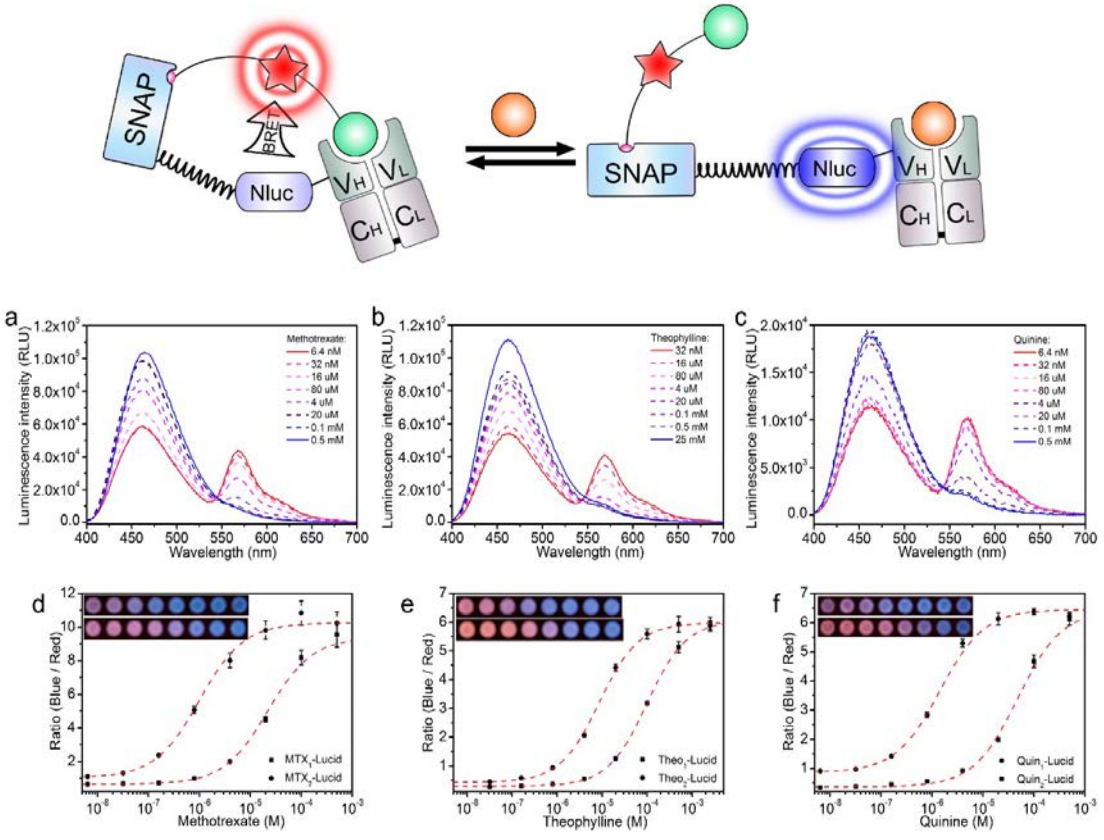

Nicotinamide adenine dinucleotides

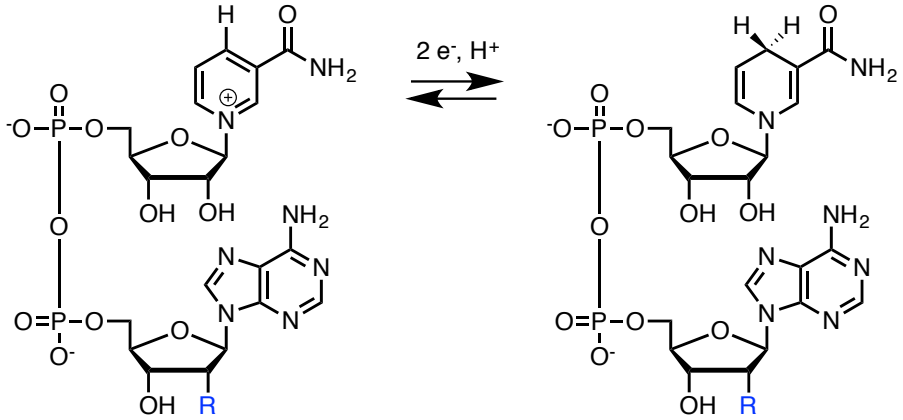

R= -OH: NAD^+, NADH

R= $-OPO_3^{2-}$: $NADP^+$, NADPH

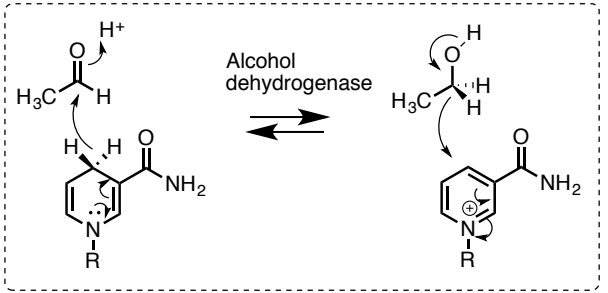

NAD⁺-dependent deacteylation of proteins through sirtuins

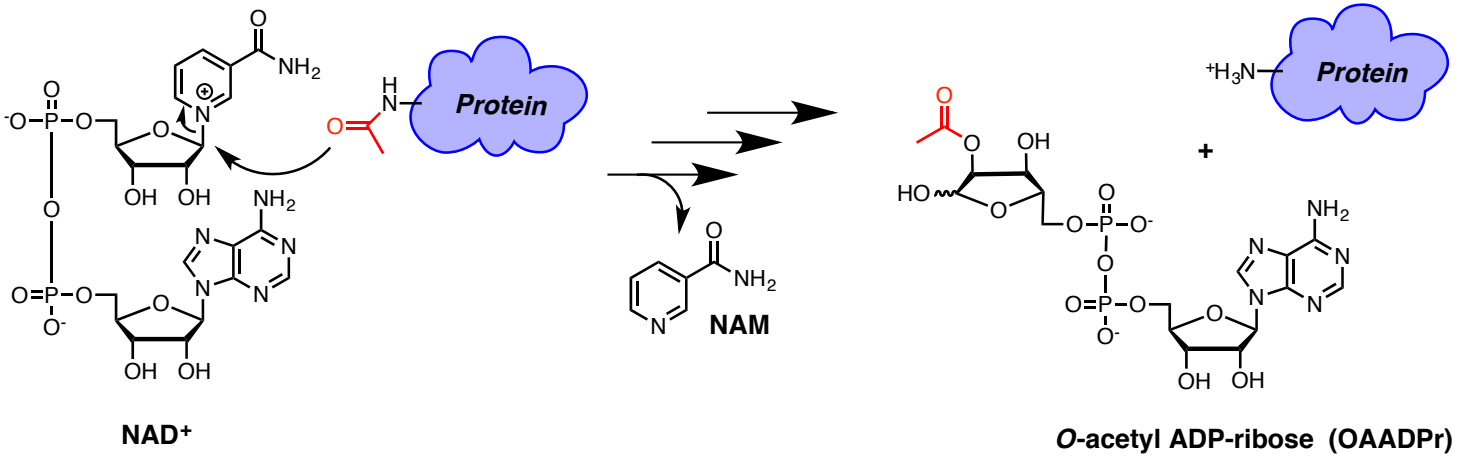

NAD⁺

***O*-acetyl ADP-ribose (OAADPr)**

NAD+ as a central cofactor and biomarker

SPECIAL SECTION *AGING*

REVIEW

NAD+ in aging, metabolism, and neurodegeneration

Eric Verdin

Nicotinamide adenine dinucleotide (NAD^+) is a coenzyme found in all living cells. It serves both as a critical coenzyme for enzymes that fuel reduction-oxidation reactions, carrying electrons from one reaction to another, and as a cosubstrate for other enzymes such as the sirtuins and poly(adenosine diphosphate–ribose) polymerases. Cellular NAD^+ concentrations change during aging, and modulation of NAD^+ usage or production can prolong both health span and life span. Here we review factors that regulate NAD^+ and discuss how supplementation with NAD^+ precursors may represent a new therapeutic opportunity for aging and its associated disorders, particularly neurodegenerative diseases.

Biosynthesis of NAD+

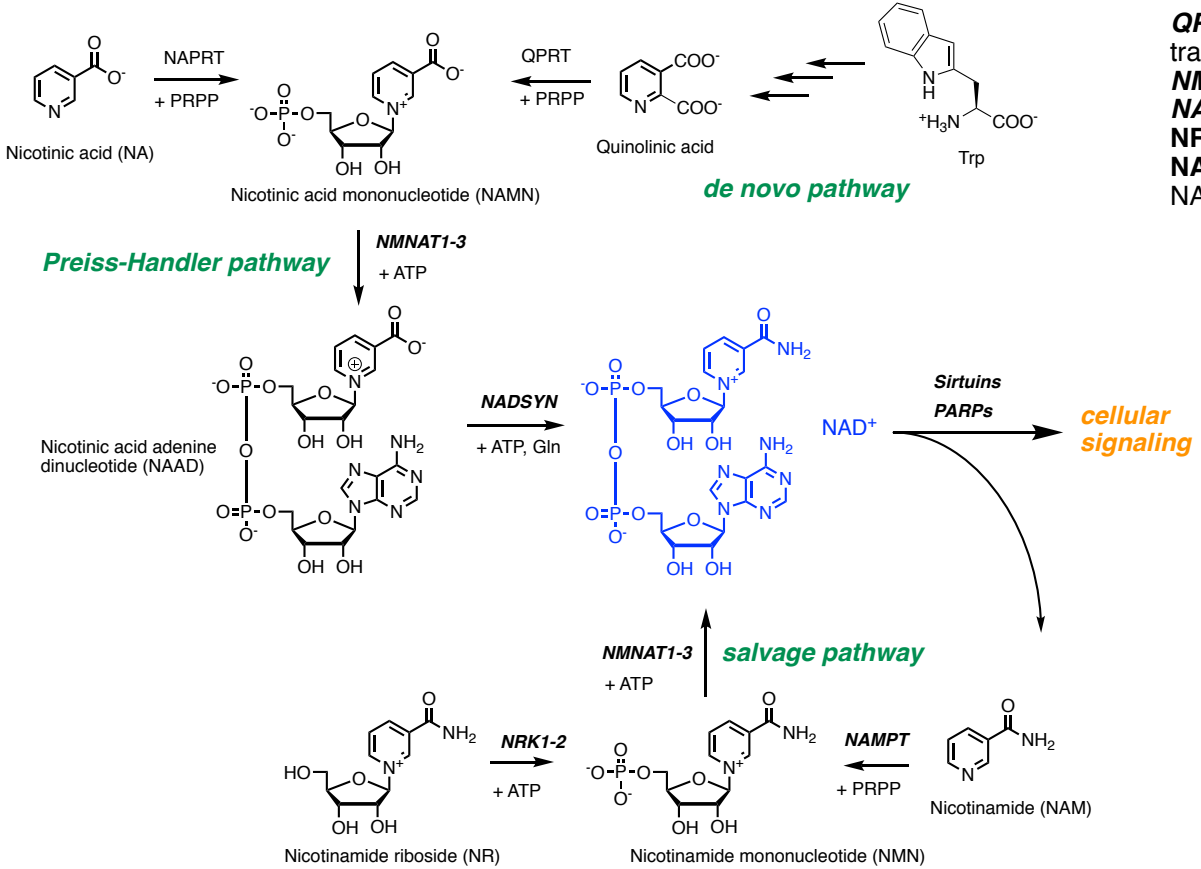

QPRT: Quinolinic acid phosphoribosyl-transferase
NMNAT: NMN adenylyltransferase
NADSYN: NAD+ synthetase
NRK: NR kinase
NAMPT: NAM phosphoribosyl-transferase
NAPRT: NA phosphoribosyl transferase

A genetically encoded sensor for [NAD⁺]

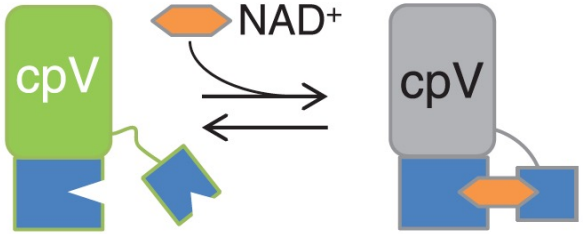

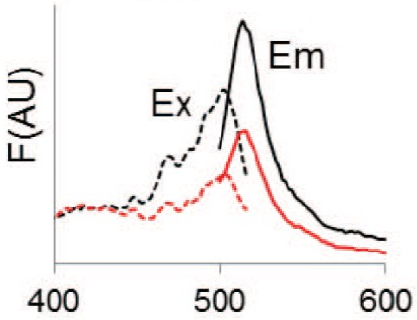

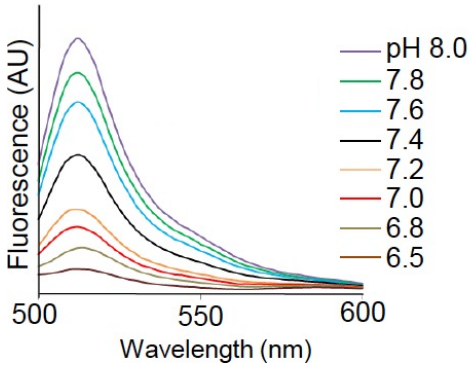

- Excited at 405/485 nm, 2 x maximum ratio change, pH sensitive
- based on a bipartite NAD⁺-binding domain from a bacterial DNA ligase

X. Cambronne *et al.*
Science **352,** 6292 (2016)

MAX-PLANCK-GESELLSCHAFT

How do generate a Snifit to measure NADPH/NADP+

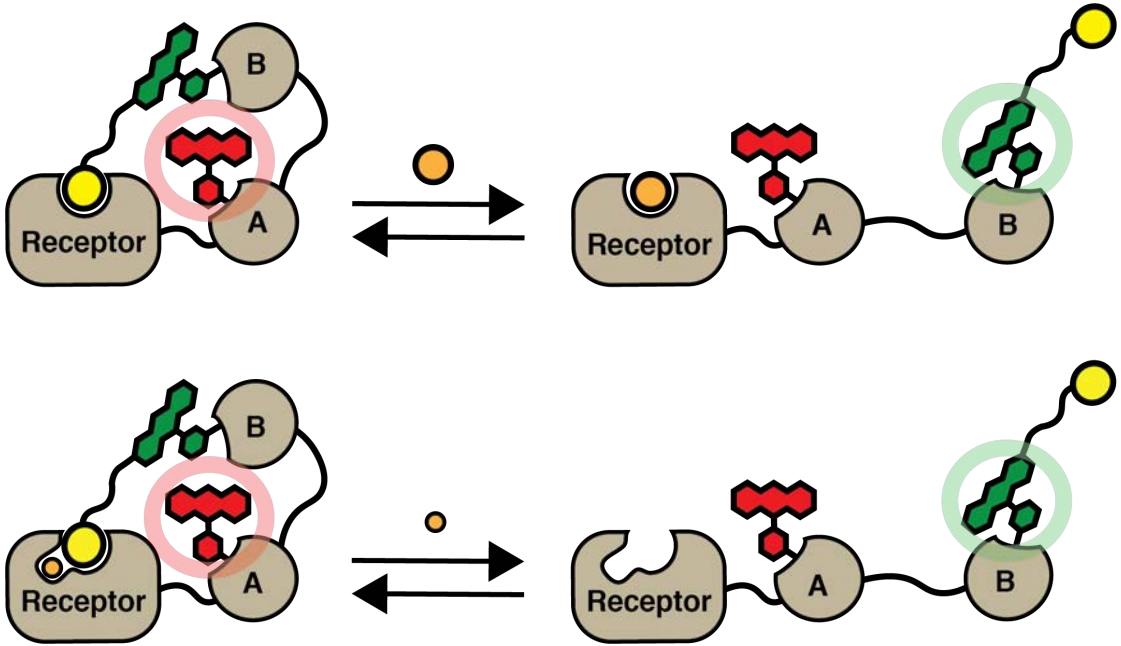

Inhibition of sepiapterin reductase (SPR) by sulfa drugs

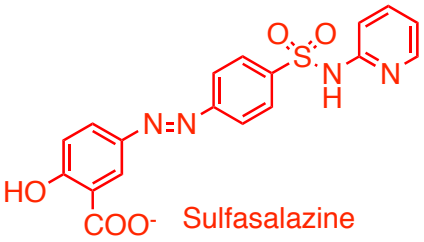

Sulfasalazine

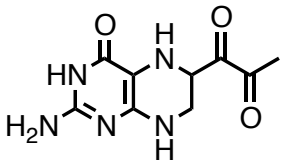

Pyruvoyltetrahydropterin

Sepiapterin reductase (SPR)

NADPH $\rightarrow$ $NADP^+$

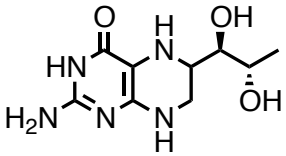

Tetrahydrobiopterin (BH_4)

Nature Chemical Biology **2011**, *7*, 375;

Binding of sulfa drugs to SPR requires the presence of $NADP^+$

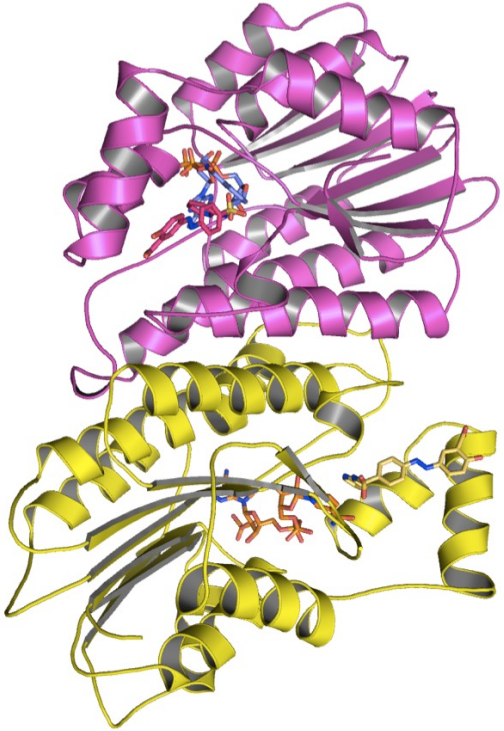

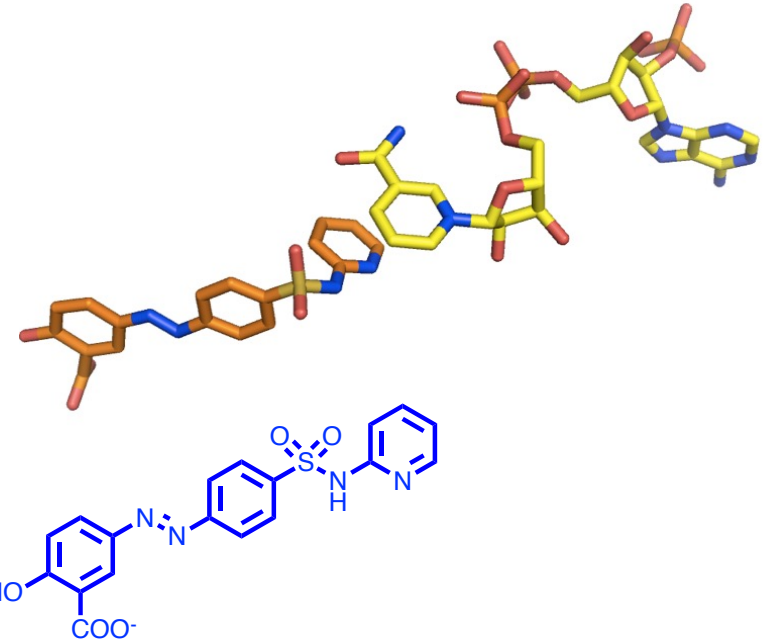

Science **2013**, *340*, 987;

NADP-Snifit: A semisynthetic biosensor for measuring NADPH/NADP+

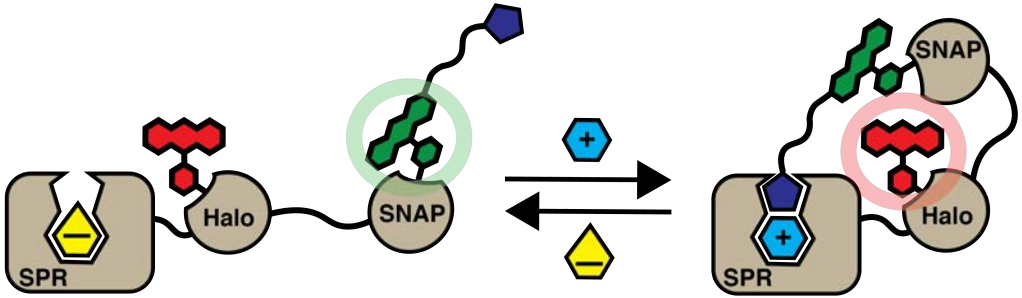

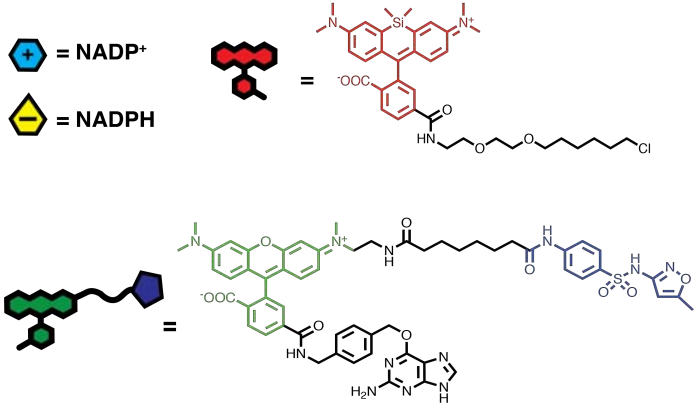

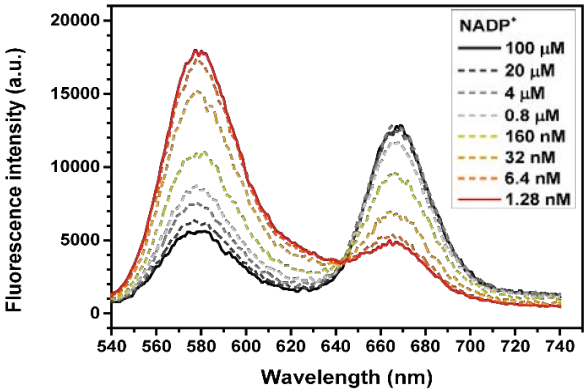

eLife 2018; 7:e32638

MAX-PLANCK-GESELLSCHAFT

NADP-Snifit: a sensor for [NADPH]/[NADP+]

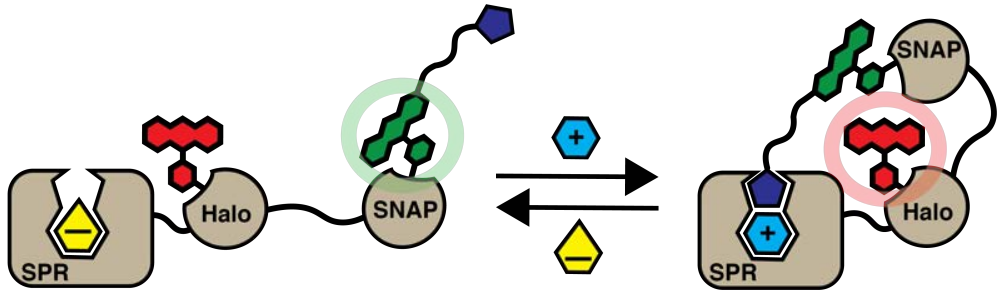

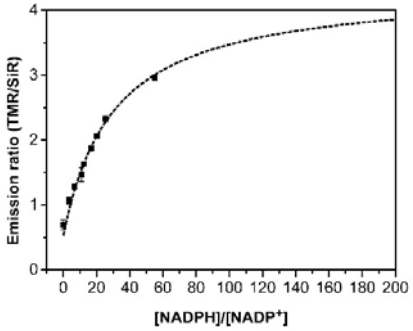

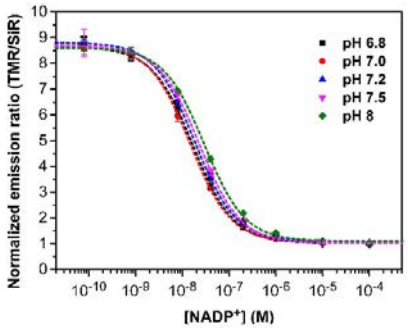

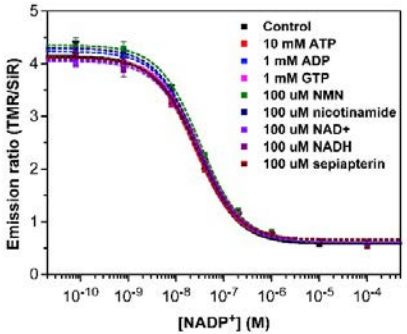

eLife 2018; 7:e32638

MAX-PLANCK-GESELLSCHAFT

Engineering NADP-Snifit into NAD-Snifit

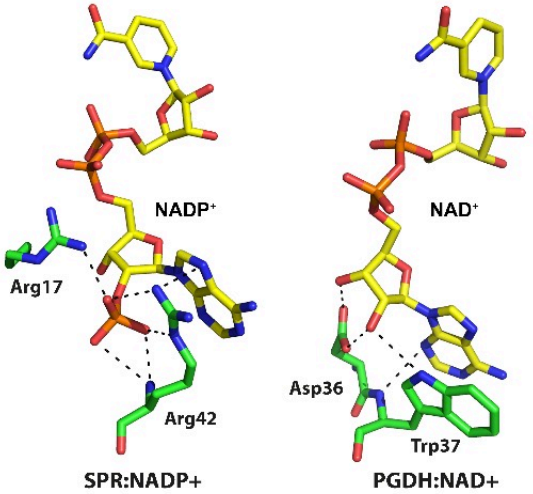

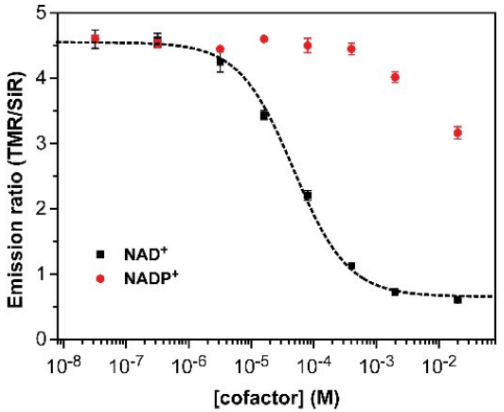

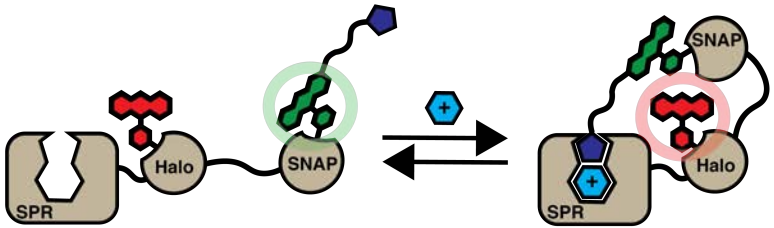

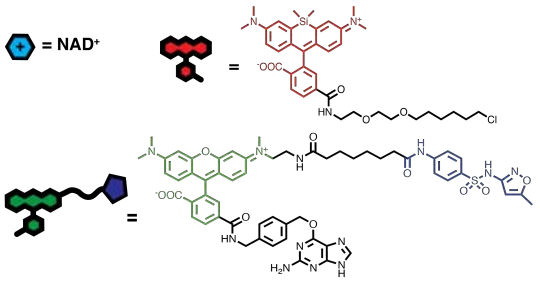

MAX-PLANCK-GESELLSCHAFT

NADP- and NAD-Snifit can be labeled in different organelles

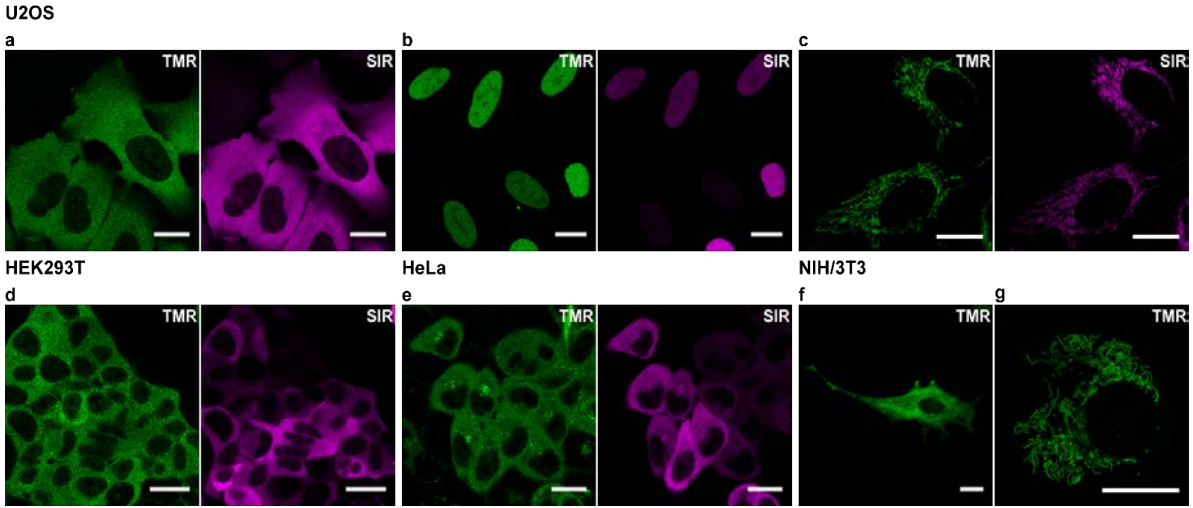

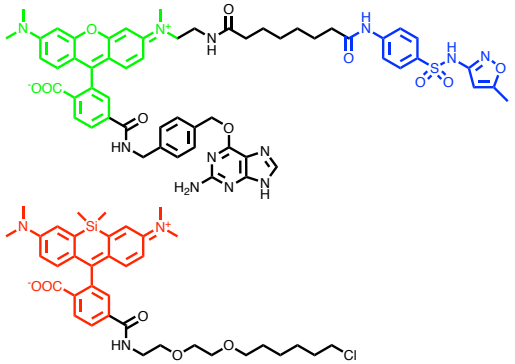

- Overnight incubation of cells with substrates results in labeling efficiencies of > 90%

eLife 2018; 7:e32638

MAX-PLANCK-GESELLSCHAFT

Quantification of free [NADPH]/[NADP$^+$] in U2OS cells

	[NADPH]/[NADP$^+$]	
	Emission ratio	TCSPC-FLIM
Cytosol	64.9 ± 26.1	55.8 ± 11.7
Nucleus	51.0 ± 16.7	40.4 ± 6.7
Mitochondria	218.7 ± 107.2	175.3 ± 57.9

eLife 2018; 7:e32638

Oxidative stress lowers free cytosolic [NADPH]/[NADP+] in U2OS cells

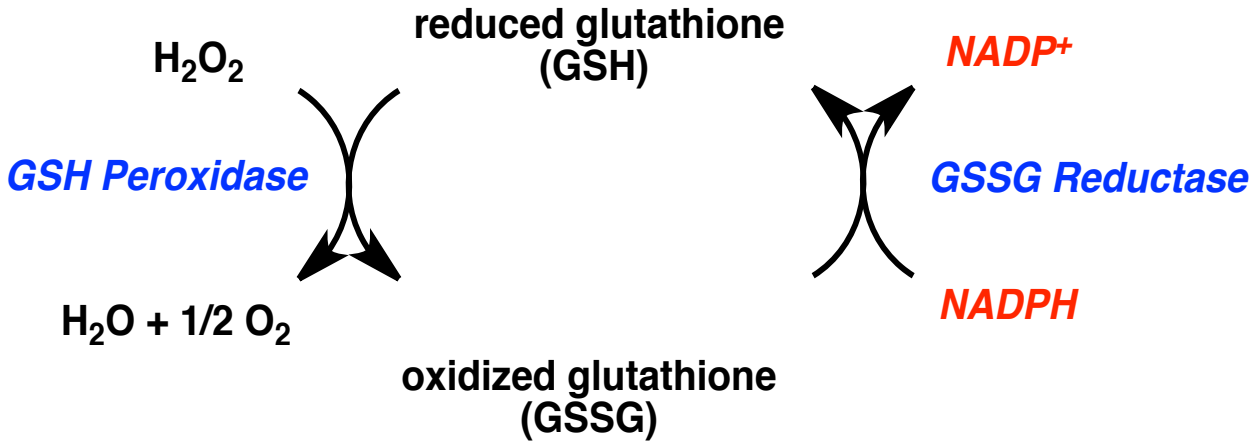

Oxidative stress lowers free cytosolic [NADPH]/[NADP+] in U2OS cells

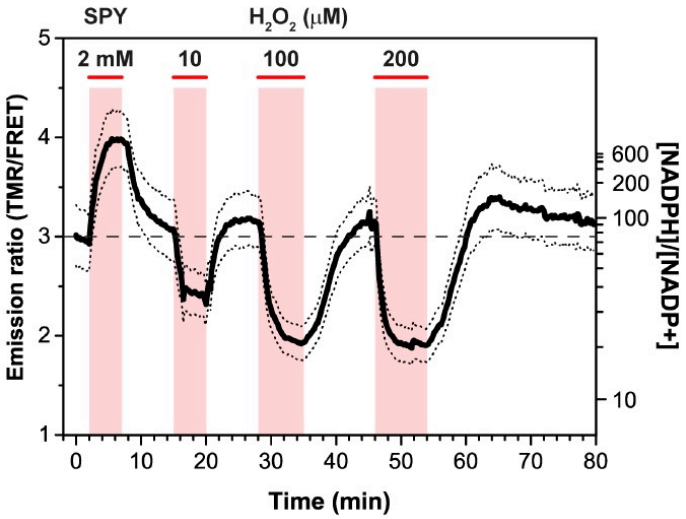

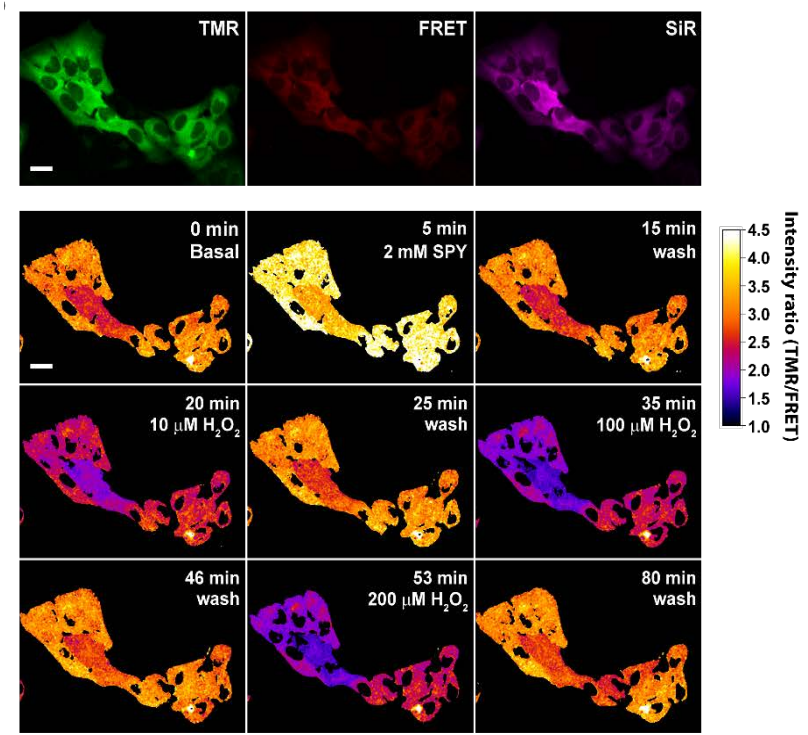

eLife 2018; 7:e32638

MAX-PLANCK-GESELLSCHAFT

Pharmacological control of [NADPH]/[NADP+] and [NAD+]

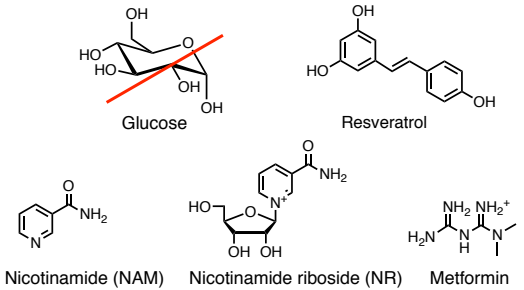

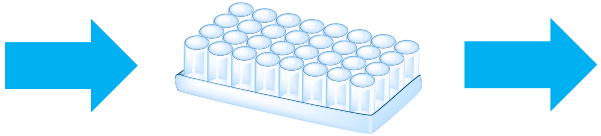

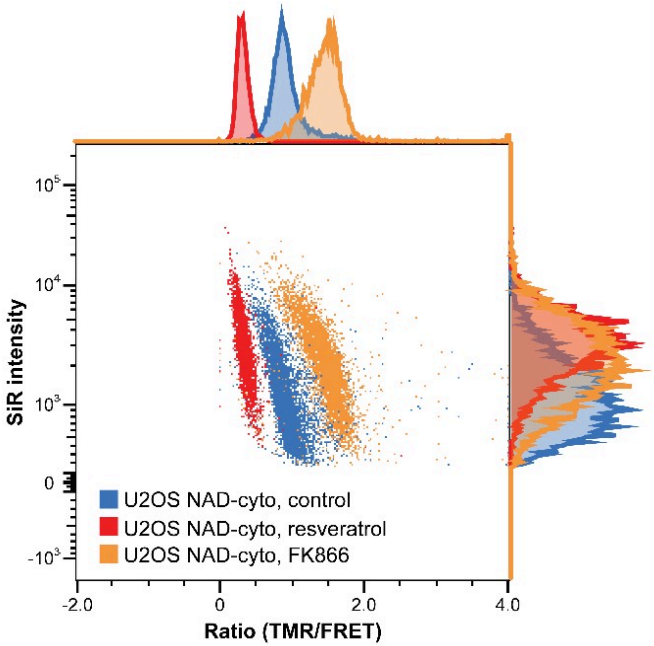

Pharmacological control of [NADPH]/[NADP+] and [NAD+]

Treatment	Normalized FRET ratio (TMR/FRET)		Normalized FRET ratio (TMR/FRET)	
	NAD-Snifit		NADP-Snifit	
	Cytosol	Mitochondria	Cytosol	Mitochondria
Control	1.00 (±0.03)	1.00 (±0.02)	1.00 (±0.01)	1.00 (±0.01)
2.5 mM glucose + 2-DG	0.68 (±0.04)	0.76 (±0.01)	0.74 (±0.01)	0.79 (±0.01)
100 uM Resveratrol	0.39 (±0.02)	0.47 (±0.01)	0.37 (±0.04)	0.40 (±0.01)
1 mM NA	0.91 (±0.01)	n.d.	0.92 (±0.01)	1.00 (±0.01)§
10 mM Nam	0.93 (±0.02)	n.d.	1.05 (±0.01)	n.d.
1 mM NMN	0.82 (±0.01)	n.d.	0.95 (±0.01)	0.99 (±0.01)§
10 mM NR	0.80 (±0.02)	n.d.	0.96 (±0.01)	1.00 (±0.01)§
100 nM FK866	1.61 (±0.06)	1.48 (±0.04)	1.05 (±0.01)	0.99 (±0.01)§
1 mM 6-AN	n.d.	n.d.	0.80 (±0.02)	n.d.
1 mM Metformin	0.89 (±0.04)	1.09 (±0.03)	0.90 (±0.01)	0.95 (±0.01)
1 mM Phenformin	0.79 (±0.05)	1.13 (±0.06)	0.88 (±0.01)	0.83 (±0.01)
10 µM Rotenone	0.67 (±0.03)	1.08 (±0.02)	0.75 (±0.02)	0.80 (±0.02)
25 µM Oligomycin	1.14 (±0.03)	1.63 (±0.01)	1.12 (±0.03)	1.36 (±0.07)

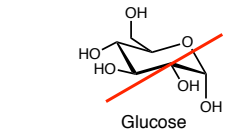

Glucose

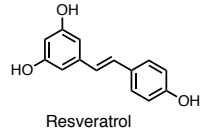

Resveratrol

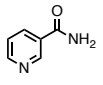

Nicotinamide (NAM)

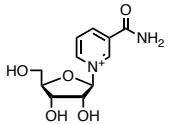

Nicotinamide riboside (NR)

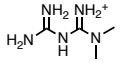

Metformin

Improving labeling of NAD(P)-Snifits

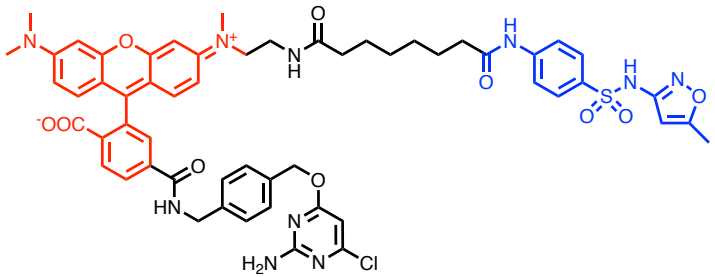

CP-TMR-C6-SMX

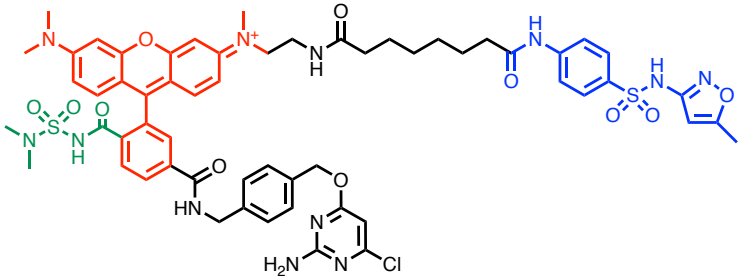

CP-MaP$_{555}$-C6-SMX

CP-TMR-C6-SMX, LP: 10%

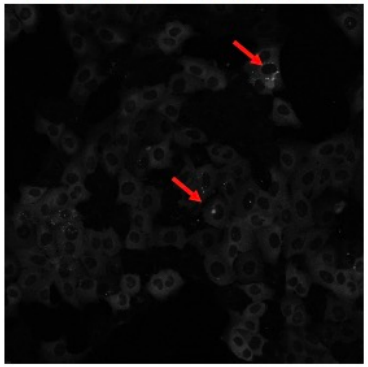

CP-MaP2-C6-SMX, LP: 5%

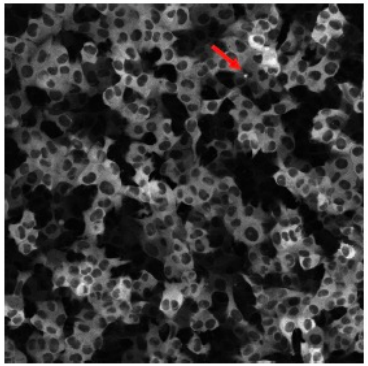

Labeling with 500 nM substrate and 200 nM Halo-SiR for 16h; U2OS cells expressing cytosolic NAD-Snifit

A genetically encoded sensor for [NAD⁺]

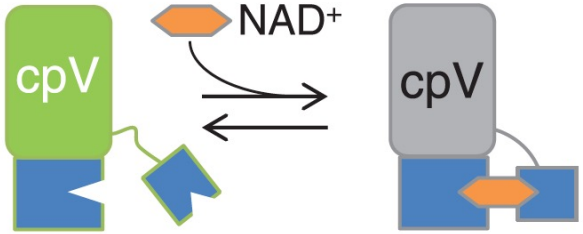

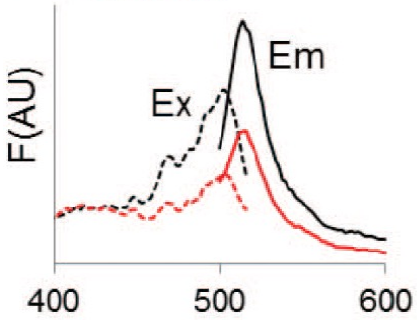

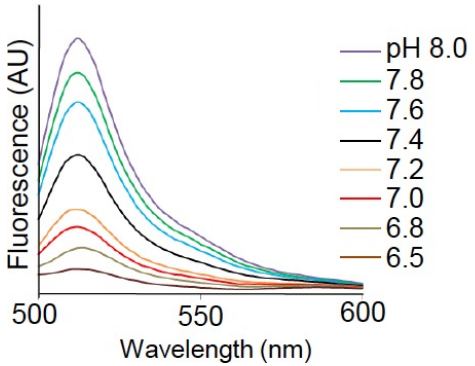

- Excited at 405/485 nm, 2 x maximum ratio change, pH sensitive
- based on a bipartite NAD⁺-binding domain from a bacterial DNA ligase

X. Cambronne *et al.*
Science **352,** 6292 (2016)

MAX-PLANCK-GESELLSCHAFT

Snifits: competitive or cooperative binding of tethered ligand

Competitive binding

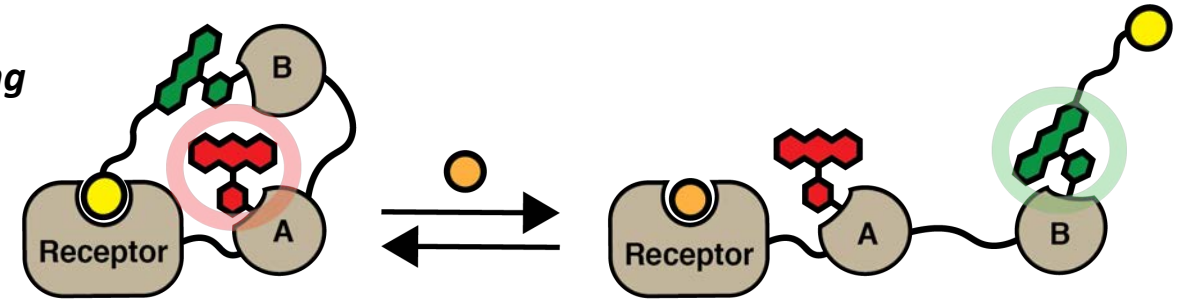

Cooperative binding

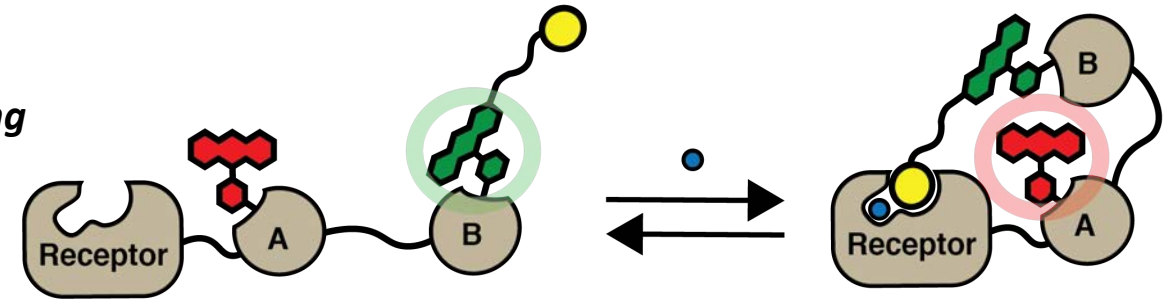

MAX-PLANCK-GESELLSCHAFT

How can we quantify biomarker and drug concentrations from a drop of blood at home?

Therapeutic Drug Monitoring

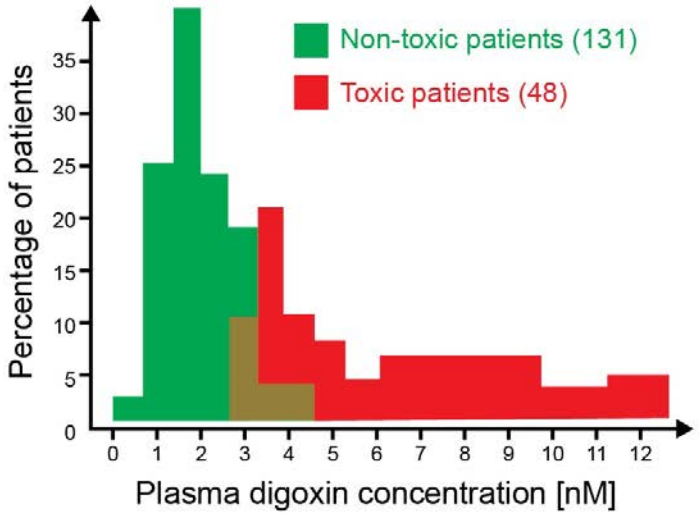

J. S. Kang, M. H. Lee, *The Korean journal of internal medicine* **24**, 1 (2009).
R. Cristodorescu, G. Deutsch, S. Dragan, *Medecine interne* **27**, 25 (1989).
W. D. Hooper, J. H. Tyrer, M. J. Eadie, *Aust Nz J Med* **4**, 449 (1974).

A suitable biosensor for POC diagnostics

- uses unprocessed samples (capillary blood, salvia or urine)
- no washing or mixing step
- no operator intervention needed
- quantitative
- automated readout by low-cost device
- device needs to be portable
- no training required

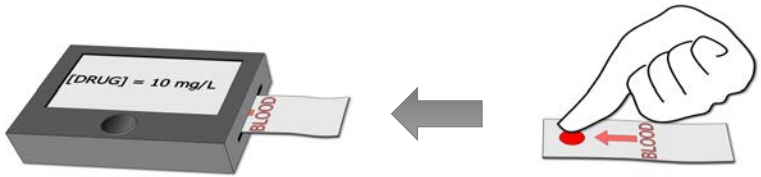

From FRET to BRET: Turning Snifits into Luciferase-based indicators

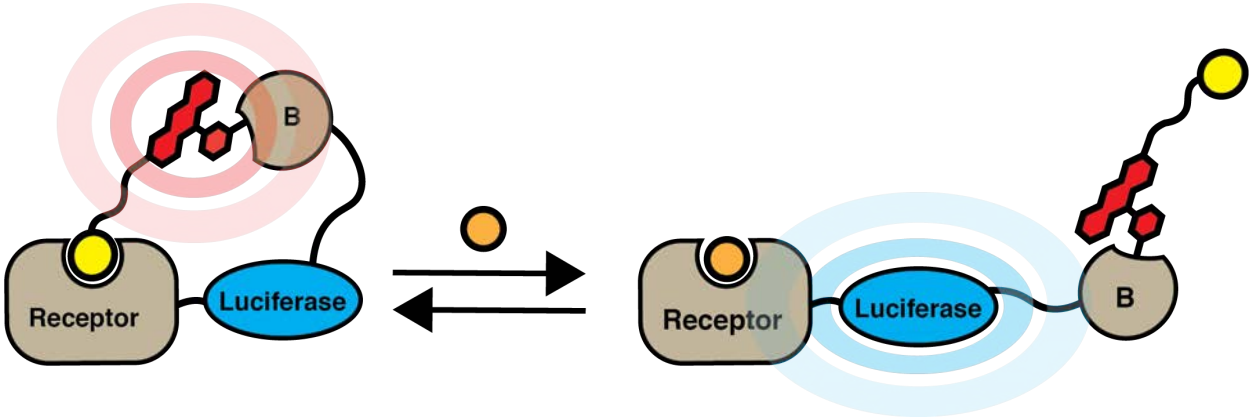

Nat Chem Biol **10**, 598 (2014)

A Snifit for methotrexate based on dihydrofolate reductase and tethered methotrexate

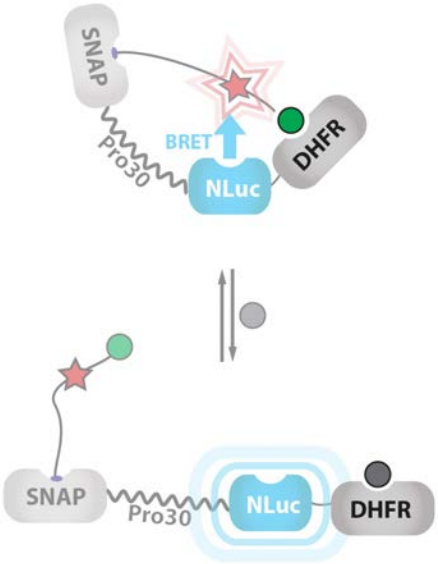

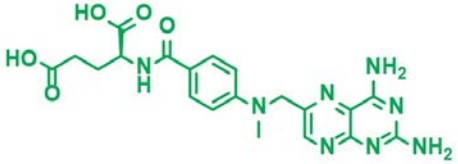

Methotrexate

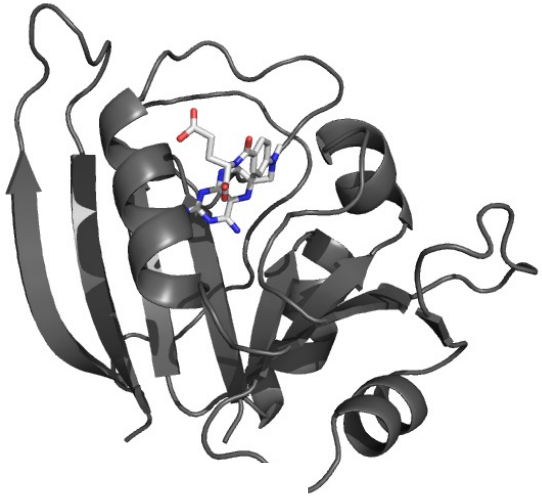

DHFR

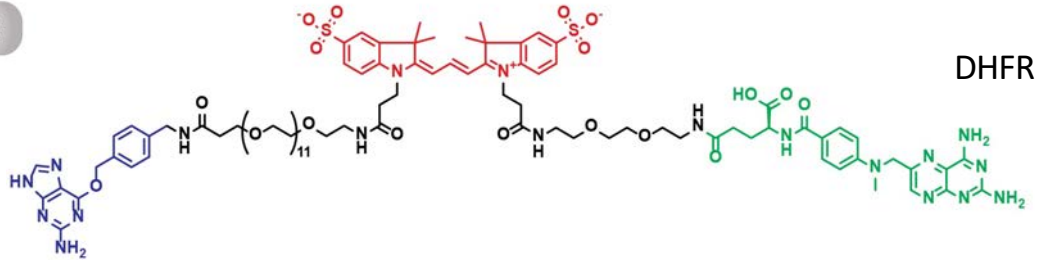

A Snifit for methotrexate based on dihydrofolate reductase and tethered methotrexate

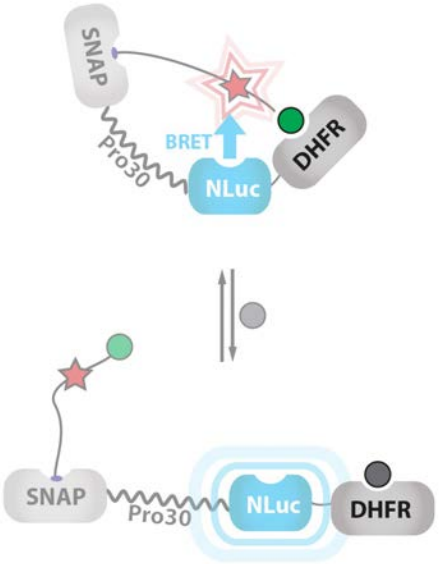

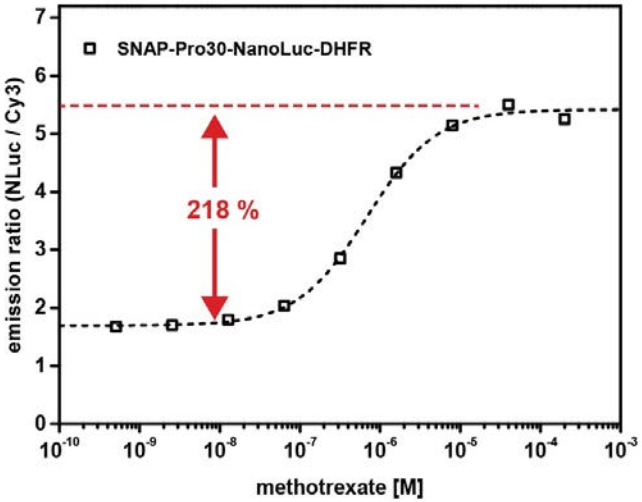

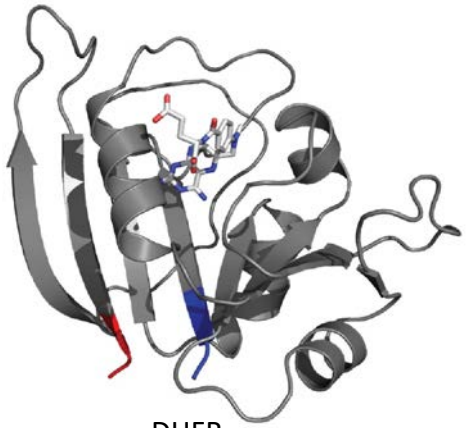

DHFR

A Snifit for methotrexate based on dihydrofolate reductase and tethered methotrexate

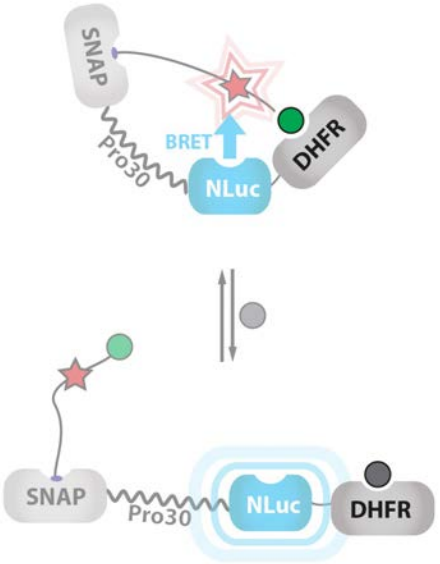

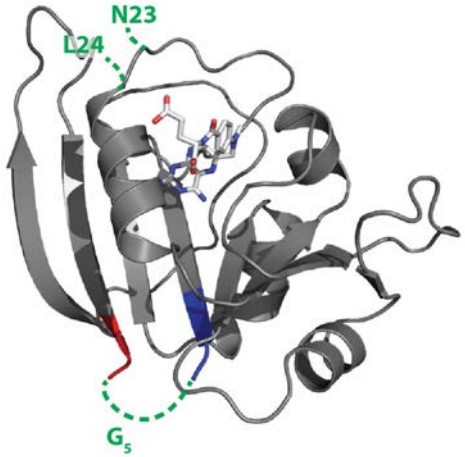

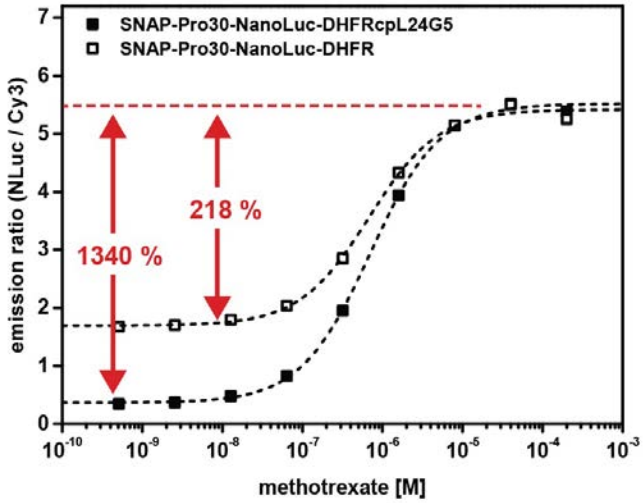

A Snifit for methotrexate based on dihydrofolate reductase and tethered methotrexate

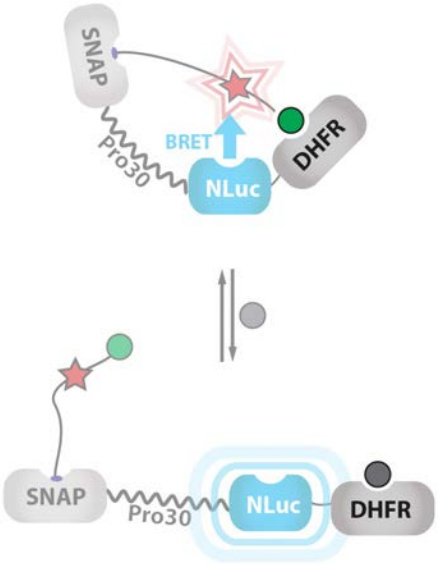

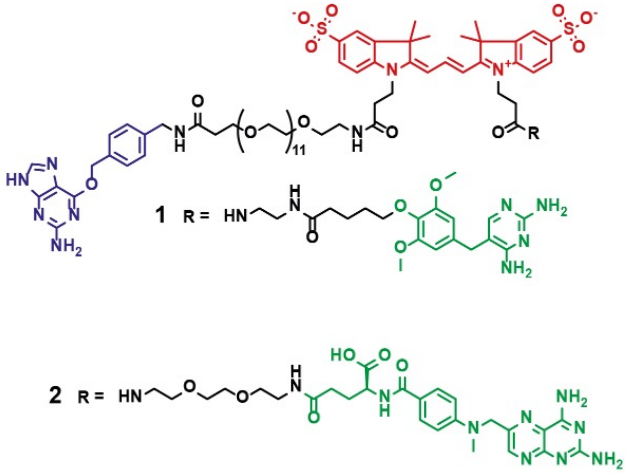

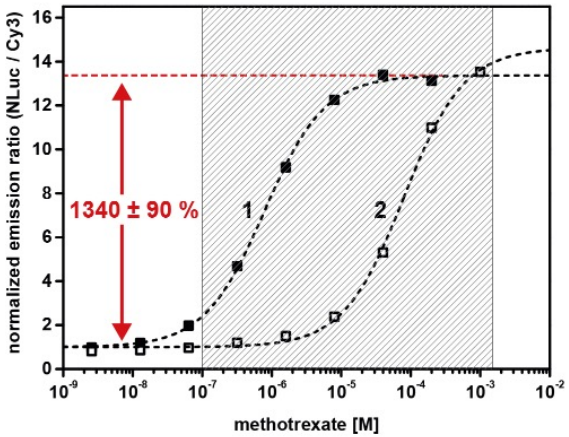

MAX-PLANCK-GESELLSCHAFT

Ratiometric sensors and matrix effects

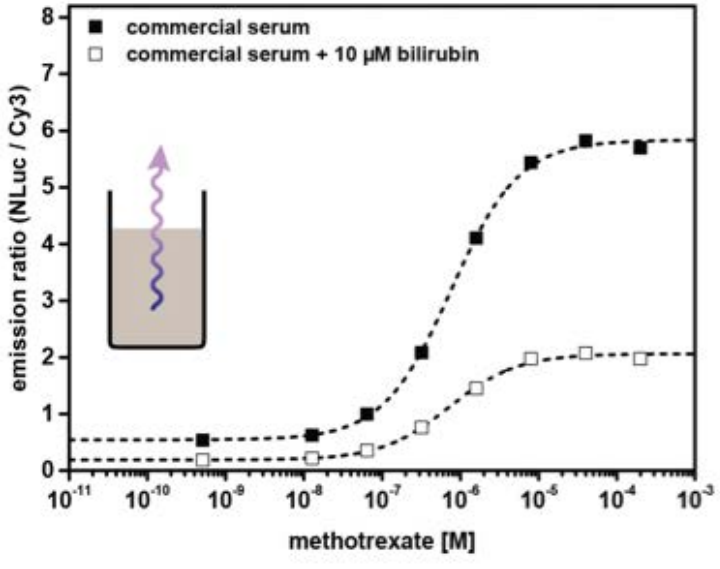

Measurement on paper reduces matrix effects

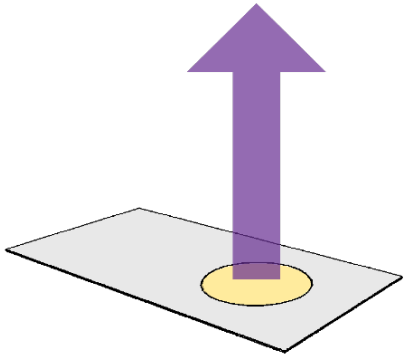

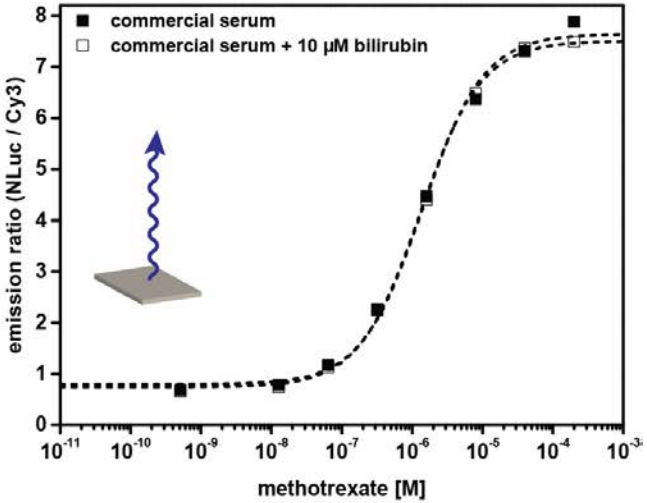

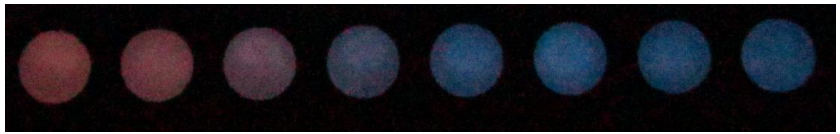

Nat Chem Biol **10**, 598 (2014)

Paper-based BRET assays

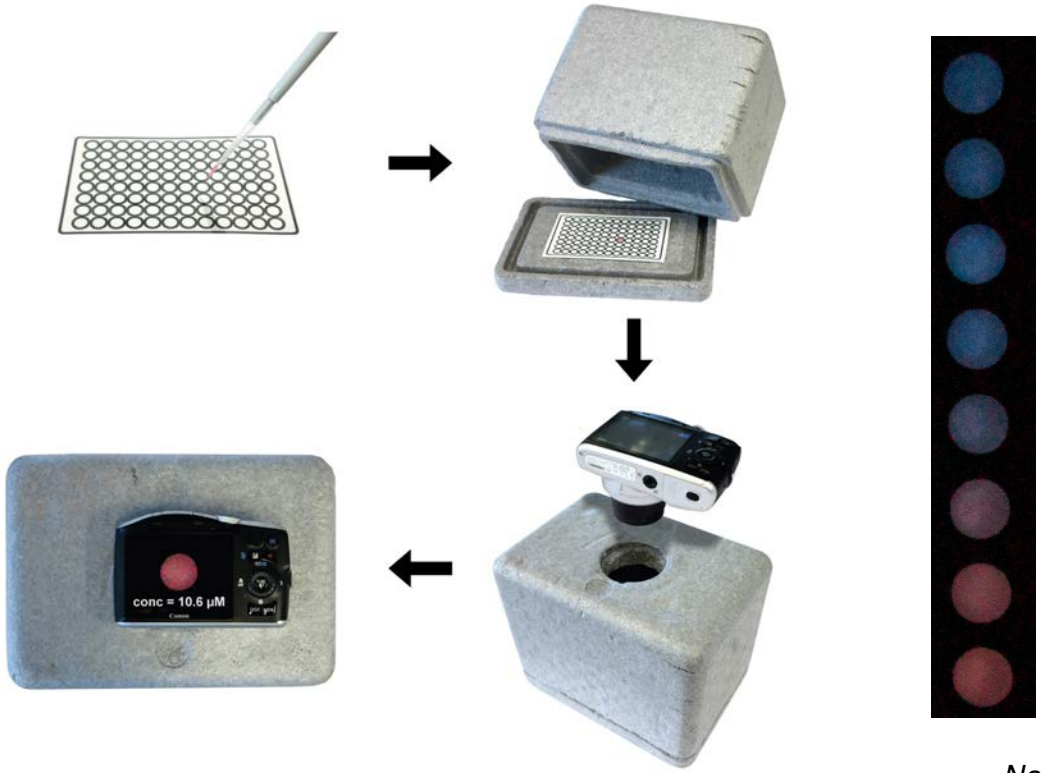

Nat Chem Biol **10**, 598 (2014)

Measuring Methotrexate in Patient Samples

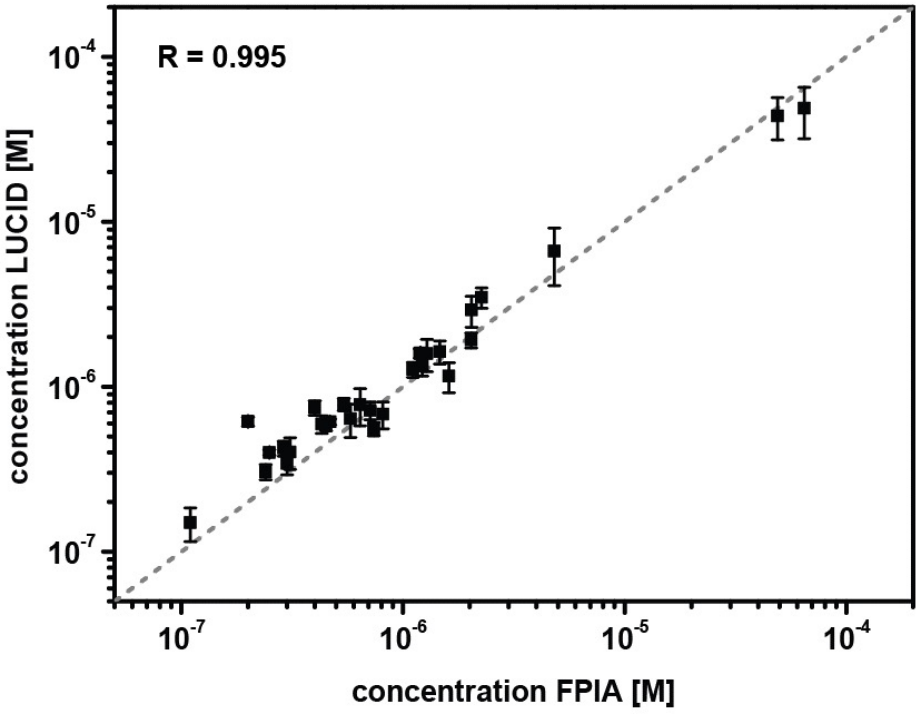

LUCID for Tacrolimus (FK506) and Sirolimus (rapamycin)

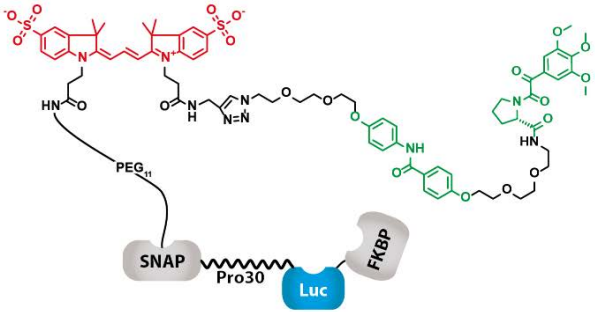

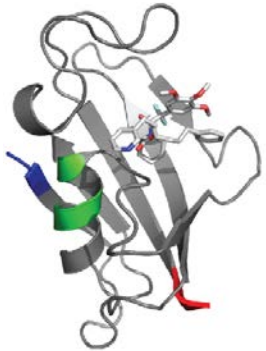

FKBP12

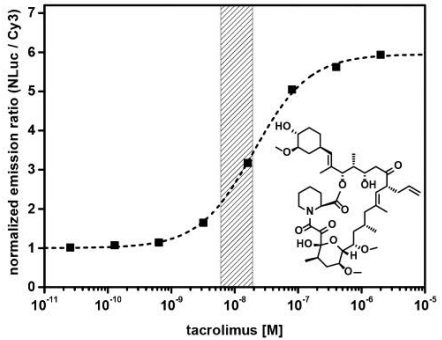

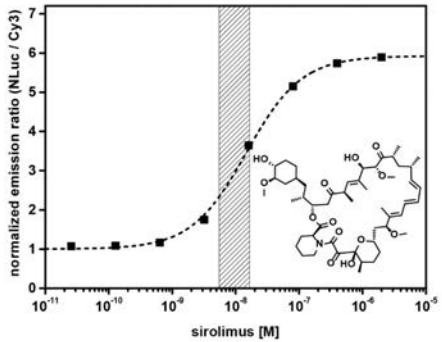

Snifits for other drugs

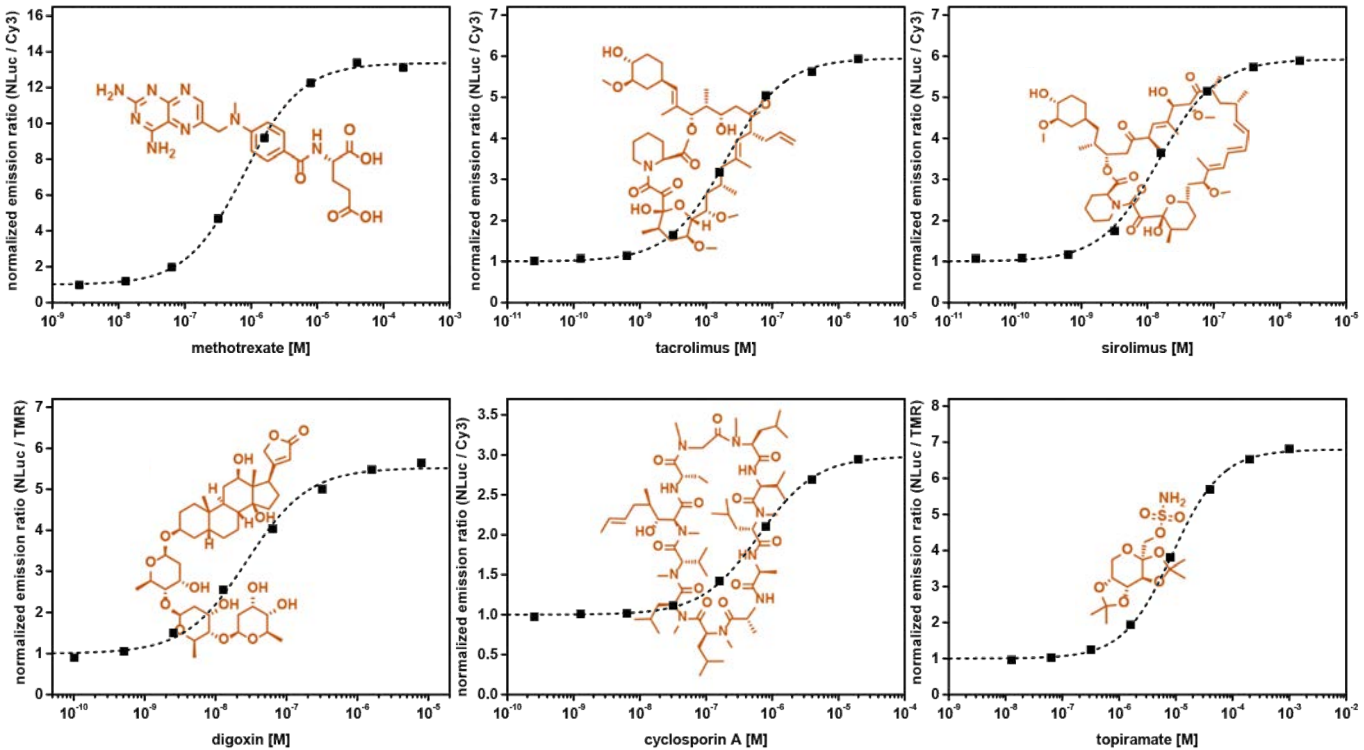

MAX-PLANCK-GESELLSCHAFT

Measuring phenylalanine at the point-of-care for phenylketonuria management

- 1/10’000 newborns diagnosed with phenylketonuria
- Phe basal level: < 80 µM; > 1200 µM in PKU patients
- Increased Phe levels during development lead to intellectual disability
- Phe levels measured in centralized labs (mass spec or chromatography)

Qiuliyang Yu, Lin Xue, Julian Hiblot, Sebastian Fabritz

Measuring phenylalanine at the point-of-care for phenylketonuria management

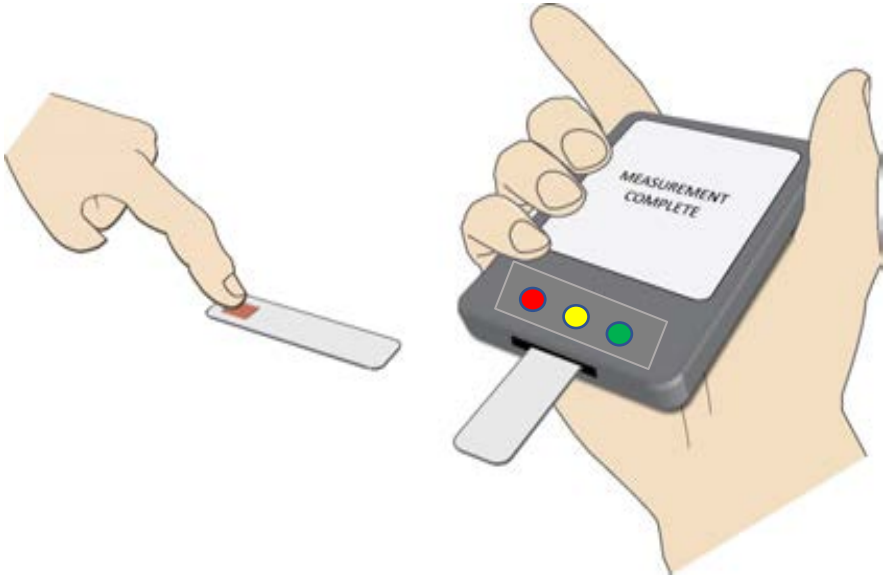

Generating a Snifit for phenylalanine

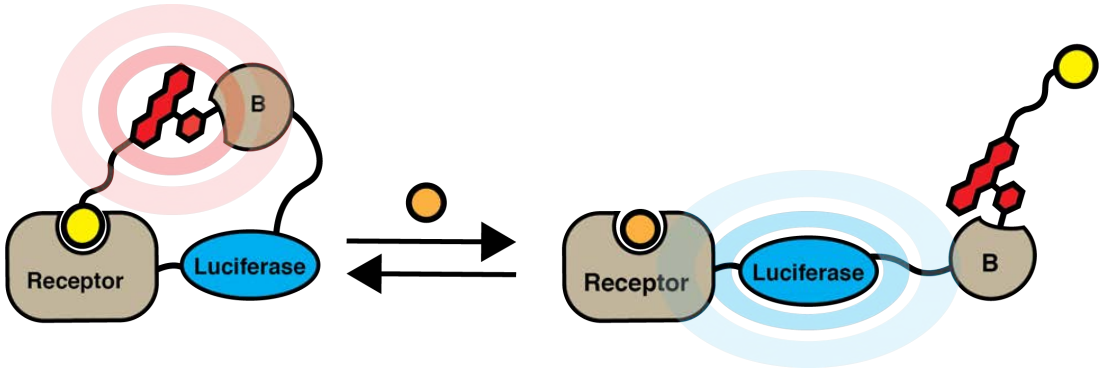

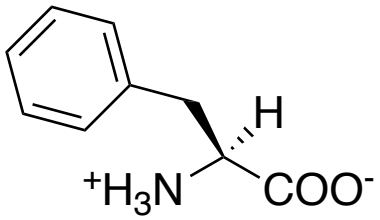

An enzymatic assay for detection of phenylalanine

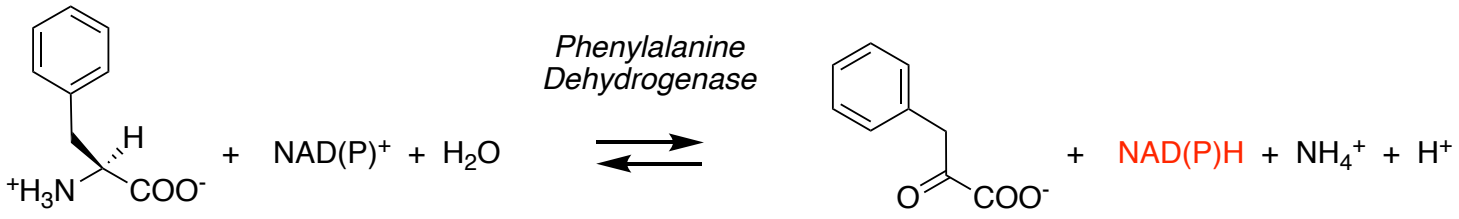

- Use of this reaction for point-of-care applications requires detection of NADPH in blood samples

A BRET sensor for NADPH based on dihydrofolate reductase

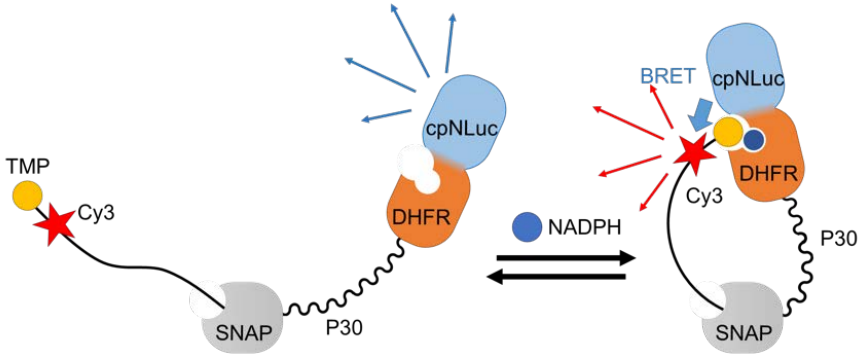

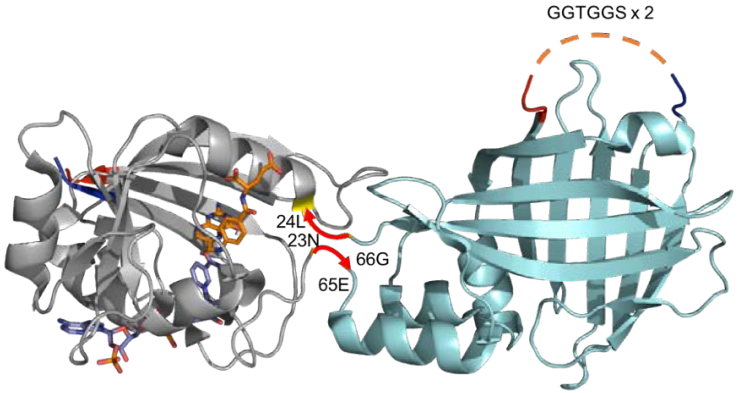

SNAP substrate

Yu et al., Science, **361,** 112, *2018*

A BRET sensor for NADPH based on dihydrofolate reductase

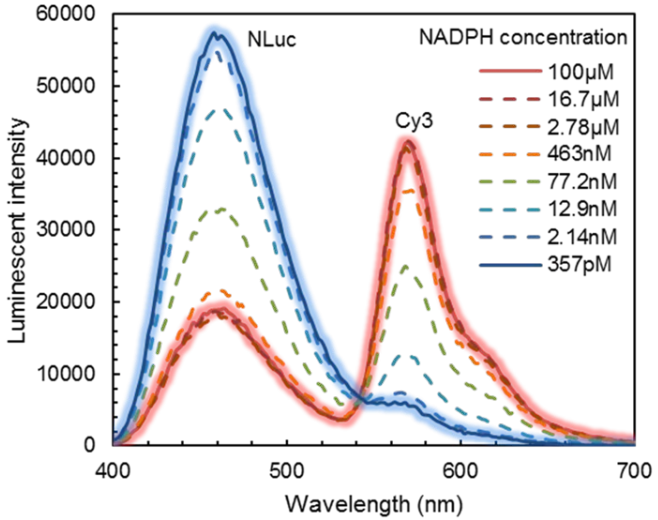

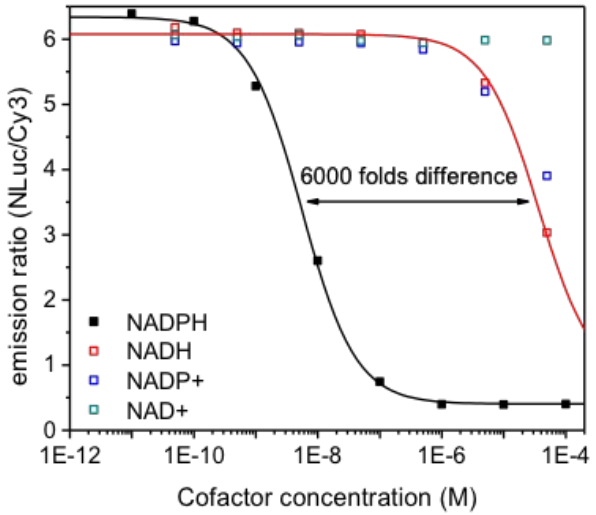

Increasing NADPH

Yu et al., Science, **361,** 112, *2018*

Engineering cooperativity into DHFR

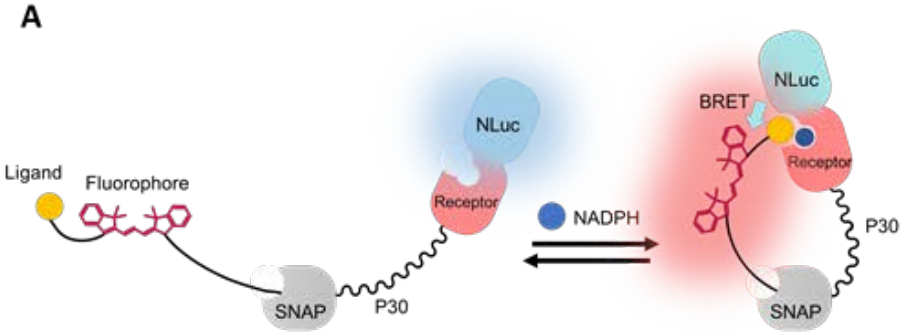

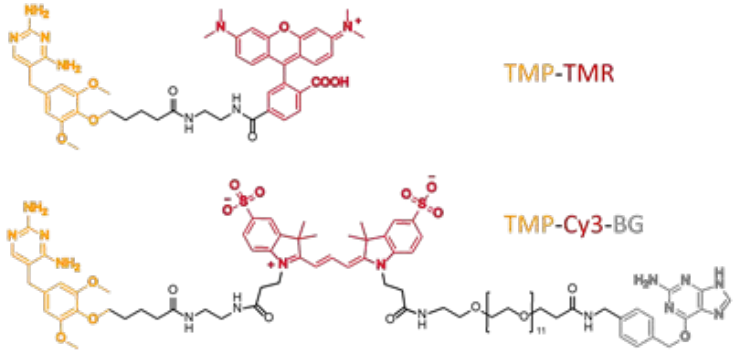

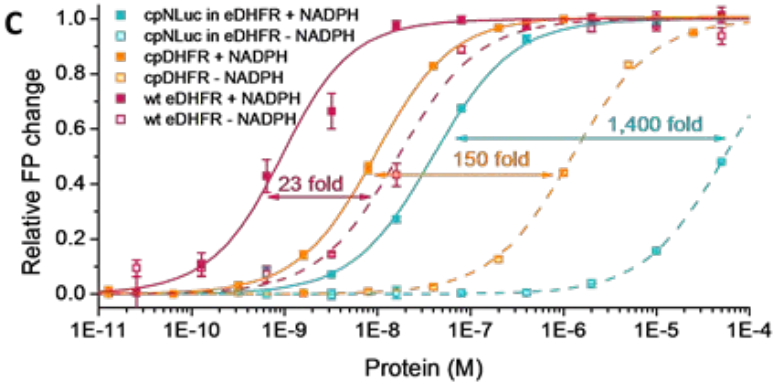

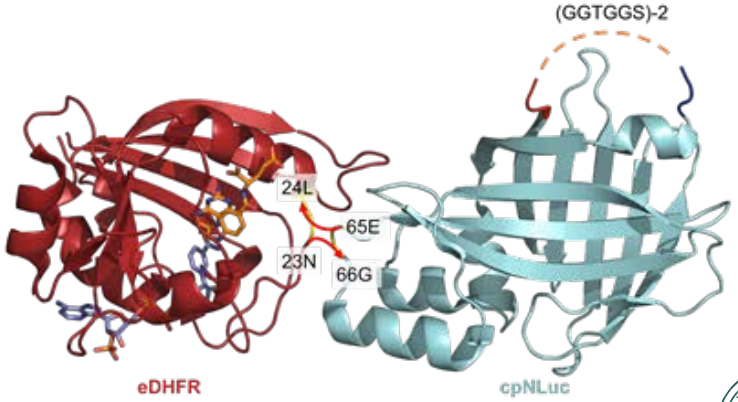

Measuring phenylalanine in unprocessed blood sampes

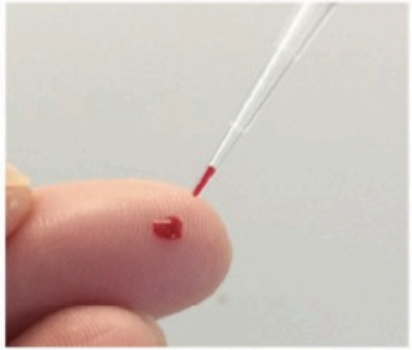

0.5 µL blood is added to 24.5 µL reaction buffer.

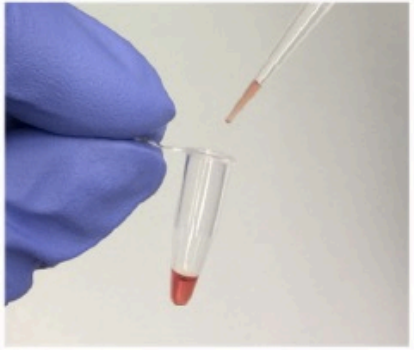

The sample is incubated for 10 minutes

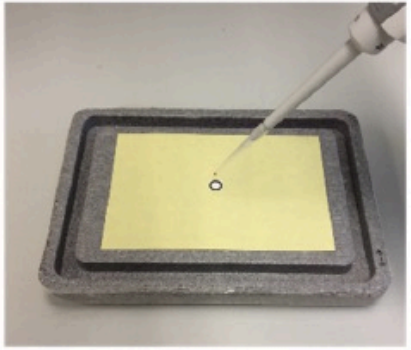

5 µL of mixture is spotted on paper containing freeze-dried sensor.

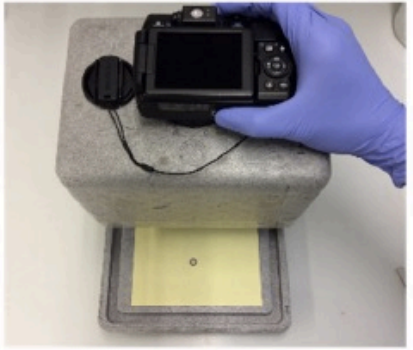

The signal is measured by digital camera.

Yu et al., Science, **361,** 112, *2018*

Validation with patient samples at University Hospital Heidelberg

8 spiked blood samples

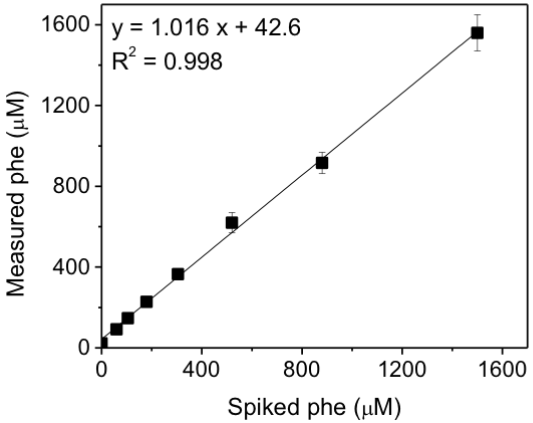

4 patient samples at the POC

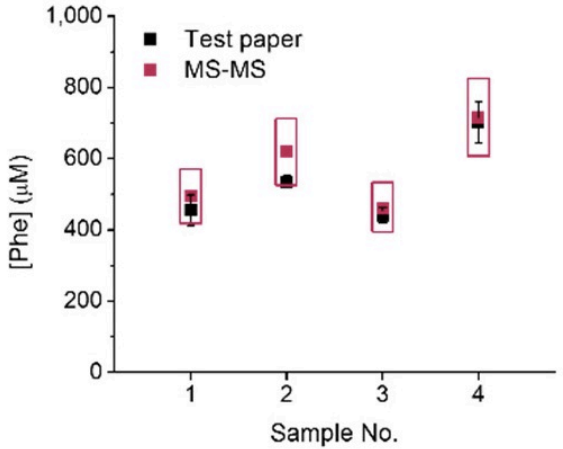

Yu et al., Science, **361,** 112, *2018*

Analytes	Normal conc.	Abnormal conc.	Sample	Medical relavance	NADP-based assay
Phenylalanine	50-80 uM	570-1023 uM	Blood	Phenylketonuria	L-Phenylalanine + H2O + NAD+ <=> Phenylpyruvate + Ammonia + NADH + H+
Glutamate	20 uM	80-156 uM	Blood	Schizophrenia	L-Glutamate + NADP+ + H2O <=> 2-Oxoglutarate + Ammonia + NADPH + H+
Glucose	3-5 mM	>10 mM	Blood	Diabetes	ATP + D-Glucose <=> D-Glucose 6-phosphate + NADP+ <=> D-Glucono-1,5-lactone 6-P + NADPH
Alanine	134-502 uM	156-1503 uM	Blood	Pearson Syndrome	L-Alanine + NAD+ + H2O <=> Pyruvate + Ammonia + NADH + H+
Leucine	136-182 uM	78-652 uM	Blood	Maple syrup urine disease	L-Leucine + H2O + NAD+ <=> 4-Methyl-2-oxopentanoate + Ammonia + NADH + H+
Tyrosine	108-196 uM	>220 uM	Blood	Tyrosinemia	L-Tyrosine + H2O + NAD+ <=> 3-(4-Hydroxyphenyl)pyruvate + Ammonia + NADH + H+
Lysine	113-269 uM	1208-1472 uM	Blood	Hyperlysinemia I	L-Lysine + NAD+ + H2O <=> L-2-Aminoadipate 6-semialdehyde + NADH + Ammonia + H+
Arginine	73-112 uM	68-422 uM	Blood	Argininemia	5-Guanidino-2-oxopentanoate + NADPH + H+ + Ammonia <=> L-Arginine + NADP+ + H2O
Glycine	147-321 uM	3464 uM	Blood	Glucoglycinuria	Glycine + H2O + NAD+ <=> Glyoxylate + Ammonia + NADH + H+
Proline	108-228 uM	208-1746 uM	Blood	Hyperprolinemia, Glutathione synthetase deficiency	L-Proline + NADP+ <=> 1-Pyrroline-2-carboxylate + NADPH + H+
Aspartate	15-27 uM	42-70 uM	Blood	Environmental enteric dysfunction	L-Aspartate + H2O + NADP+ <=> Oxaloacetate + Ammonia + NADPH + H+
Galactose	40-140 uM	921-2070 uM	Blood	Galactosemia	D-Galactose + NADP+ <=> D-Galactono-1,5-lactone + NADPH + H+
Fructose	8 uM	8-16 uM	Blood	Diabetes	D-Fructose + NADP+ <=> 5-Dehydro-D-fructose + NADPH + H+
Lactate	500-2200 uM	1200-13000 uM	Blood	Pyruvate dehydrogenase deficiency	D-Lactate + NAD+ <=> Pyruvate + NADH + H+
Cholesterol	4500-6700 uM	13000-15000 uM	Blood	Cholesterol stones	Cholesterol + NADP+ <=> Desmosterol + H+ + NADPH
Bilirubin	13-17 uM	47-233 uM	Blood	Infantile Liver Failure	Bilirubin + NADP+ <=> Biliverdin + NADPH + H+
Ammonia	15-45 uM	140-503 uM	Blood	Mitochondrial trifunctional protein deficiency	Ammonia + 3 NADP+ + 2 H2O <=> Nitrite + 3 NADPH + 3 H+
Carnitine	25-88 uM	22000-50000 uM	Blood	3-Hydroxy-3-Methylglutaryl-CoA Synthase Deficiency	Carnitine + NAD+ <=> 3-Dehydrocarnitine + NADH + H+
Xanthine	<1 uM	40-118 uM	Blood	Lesch-Nyhan syndrome, Xanthinuria,	Xanthine + NAD+ + H2O <=> Urate + NADH + H+
Acetoacetate	10-80 uM	50-1280 uM	Blood	2-Ketoglutarate dehydrogenase complex deficiency	Coenzyme M + Acetoacetate + NADP+ <=> 2-Oxopropyl-CoM + CO2 + NADPH + H+
Hydroxyproline	16-53 uM	340 uM	Blood	Hydroxyprolinemia	Hydroxyproline + NADP+ <=> 4-Oxoproline + NADPH + H+
Glycerate	0-24 uM	186-315 uM	Blood	D-Glyceric acidura	D-Glycerate + NADP+ <=> Hydroxypyruvate + NADPH + H+
Ethanol	0-80 uM	10-170 uM	Blood	Chronic renal insufficiency	Ethanol + NADP+ <=> Acetaldehyde + NADPH + H+
Glycolate	50-123 uM	0 uM	Blood	Branched-chain Keto Acid Dehydrog. Kinase Def.	Glycolate + NADP+ <=> Glyoxylate + NADPH + H+
Tryptophan	62-94 uM	30-34 uM	Blood	Epilepsy	L-Tryptophan + NADP+ + H2O <=> Indolepyruvate + Ammonia + NADPH + H+
Ascorbate	18-54 uM	0-130 uM	Blood	Hyperoxalemia	NAD+ + 2 Ascorbate <=> NADH + 2 Monodehydroascorbate + H+
4-Hydroxybutanoate	0-96 uM	2110-2920 uM	Blood	Succinic semialdehyde dehydrogenase deficiency	4-Hydroxybutanoic acid + NADP+ <=> Succinate semialdehyde + H+ + NADPH
3-Hydroxybutanoate	40-80 uM	1800 uM	Blood	Pyruvate dehydrogenase phosphatase deficiency	3-Hydroxybutanoate + NAD+ <=> Acetoacetate + NADH + H+
Salicylate	Expected but not quantified	1680 uM	Blood	Mitochondrial complex I deficiency	Benzoate + NADPH + Oxygen <=> Salicylate + NADP+ + H2O
D-Arabitol	0-5 uM	32 - 198 uM	Blood	Ribose-5-Phosphate Isomerase Deficiency	D-Arabitol + NADP+ <=> D-Xylulose + NADPH + H+
Triglyceride	<150mg/dL	>200mg/dL	Blood	Cardiovescular risk, hypothyroidism	Triglycerides + H2O <=> glycerol + free fatty acids, Glycerol + NADP+ <=> D-Glyceraldehyde + NADPH
2-Hydroxyadipate	0-20 umol/mmol creatinine	80-170 umol/mmol creatinine	Urine	alpha-Aminoadipic aciduria	2-Oxoadipate + NADH + H+ <=> 2-Hydroxyadipate + NAD+
2-Hydroxybutanoate	1-7 umol/mmol creatinine	250 umol/mmol creatinine	Urine	Dihydrolipoamide Dehydrogenase Deficiency	2-Hydroxybutanoic acid + NAD+ <=> 2-Oxobutanoate + NADH + H+
2-Hydroxyglutarate	13-78 umol/mmol creatinine	630-1420 umol/mmol creatinine	Urine	L-2-hydroxyglutaric aciduria	2-Hydroxyglutarate + NAD+ <=> 2-Oxoglutarate + NADH + H+
Succinate	1-16 umol/mmol creatinine	749-784 umol/mmol creatinine	Urine	D-2-hydroxyglutaric aciduria	Succinate + NAD+ <=> Fumarate + NADH + H+
5,6-Dihydrouracil	2-8 umol/mmol creatinine	630 umol/mmol creatinine	Urine	Dihydropyrimidine dehydrogenase (DPD) deficiency	5,6-Dihydrouracil + NADP+ <=> Uracil + NADPH + H+
Trimethylamine	<10 umol/mmol creatinine	90-320 umol/mmol creatinine	Urine	Trimethylaminuria	Trimethylamine + NAD+ + H2O <=> Trimethylamine N-oxide + NADH + H+
Hypoxanthine	4-10 umol/mmol creatinine	60-140 umol/mmol creatinine	Urine	Xanthinuria type 1	Hypoxanthine + NAD+ + H2O <=> Xanthine + NADH + H+
D-Threitol	0-7 uM	30-70 uM	CSF	Ribose-5-Phosphate Isomerase Deficiency	D-Threitol + NADP+ <=> D-Erythrulose + NADPH + H+
D-Ribose	0-5 uM	50-150 uM	CSF	Ribose-5-phosphate isomerase deficiency	D-Ribose + NADP+ + H2O <=> D-Ribonate + NADPH + H+
Xylitol	0-5 uM	30-100 uM	CSF	Ribose-5-Phosphate Isomerase Deficiency	Xylitol + NADP+ <=> D-Xylose + NADPH + H+
Nitrite	1-2 uM	20 uM	CSF	Preeclampsia	Nitrite + NADP+ + H2O <=> Nitrate + NADPH + H+

One biosensor for many metabolic assays

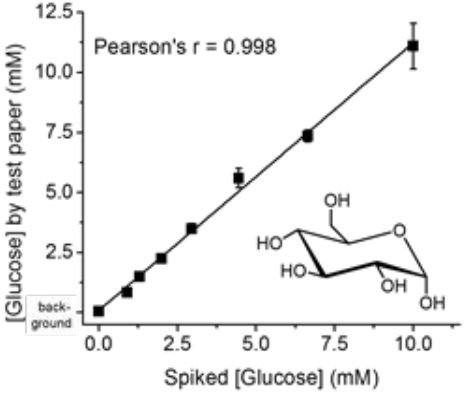

glucose + ATP <=> glucose-6-phosphate + ADP (Hexokinase)

G6P + $NADP^+$ <=> 6-phospho-D-glucono-1,5-lactone + NADPH + H^+ (G6P dehydrogenase)

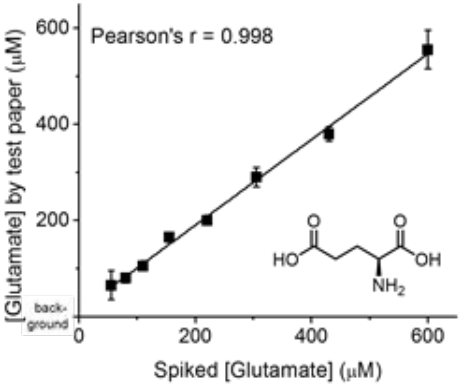

glutamate + $NADP^+$ <=> ketoglutarate + NADPH (Glutamate dehydrogenase)

Yu et al., Science, **361,** 112, *2018*

MAX-PLANCK-GESELLSCHAFT

Multiplexing

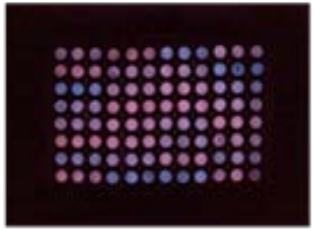

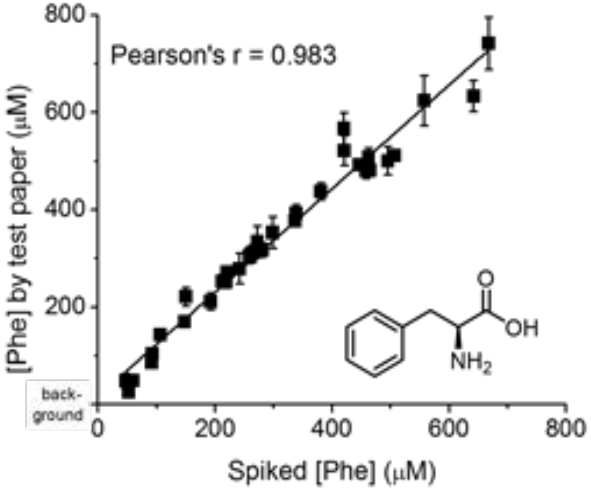

Yu et al., Science, **361,** 112, *2018*

Measuring phenylalanine levels with smartphones

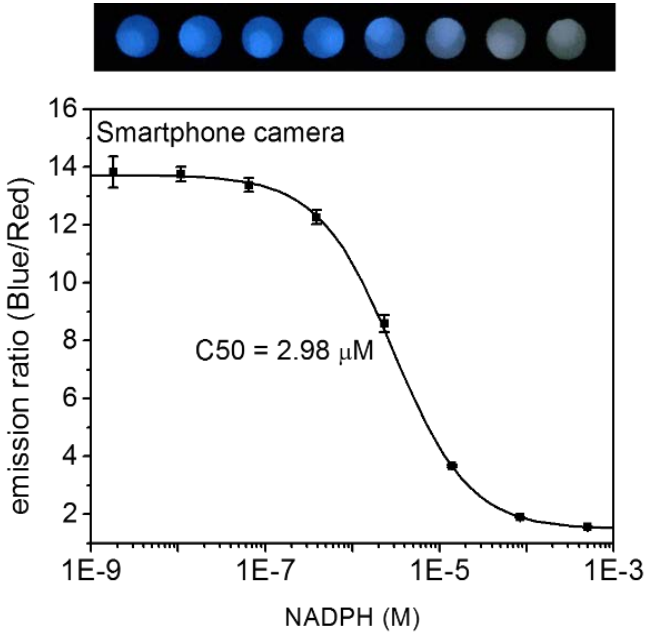

MAX-PLANCK-GESELLSCHAFT

However

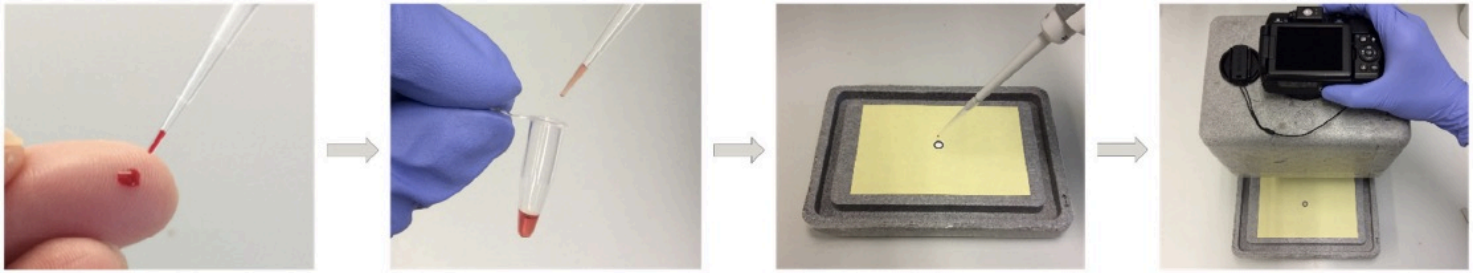

≠

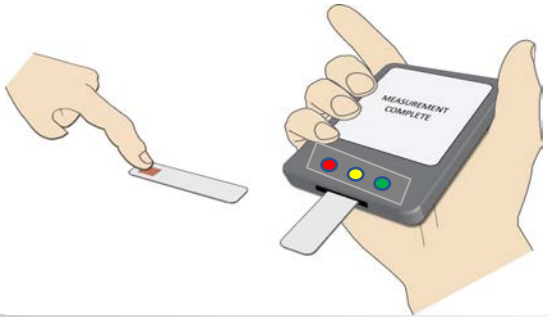

MAX-PLANCK-GESELLSCHAFT

Acknowledgements

Sebastian Fabritz

Corentin Gondrand

Rudolf Griss

Julien Hiblot

Birgit Koch

Fabio Raith

Luc Reymond

Olivier Sallin

Alberto Schena

Lin Xue

Qiuliyang Yu

Clothilde Roux; University Lausanne

Pierre-Alain Binz; University Lausanne

Dorothea Haas; University Heidelberg

Jürgen Okun; University Heidelberg

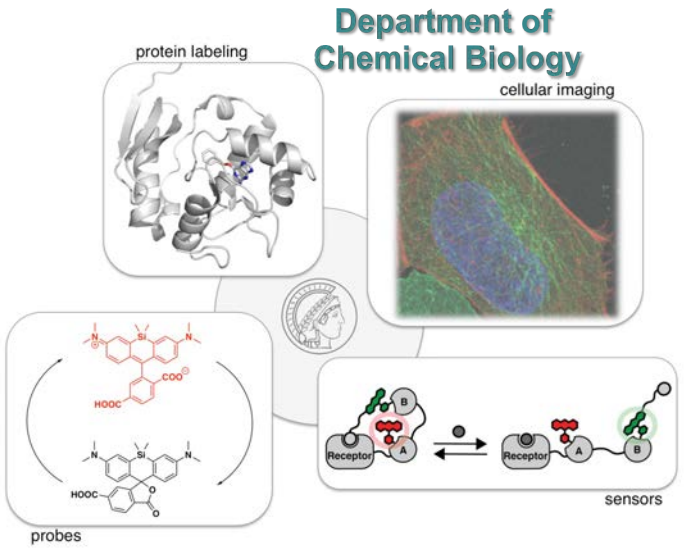

MAX-PLANCK-GESELLSCHAFT